PJNM

Philippine Journal of Nuclear Medicine

Vol. 16 No. 2 July to December 2021

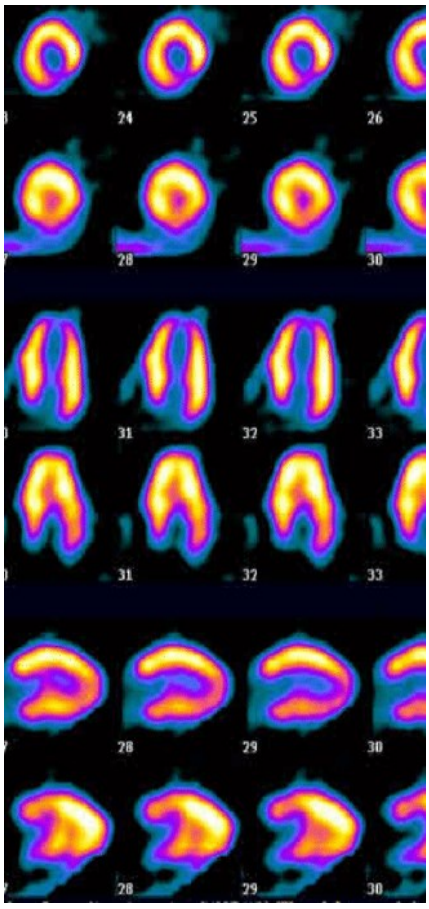

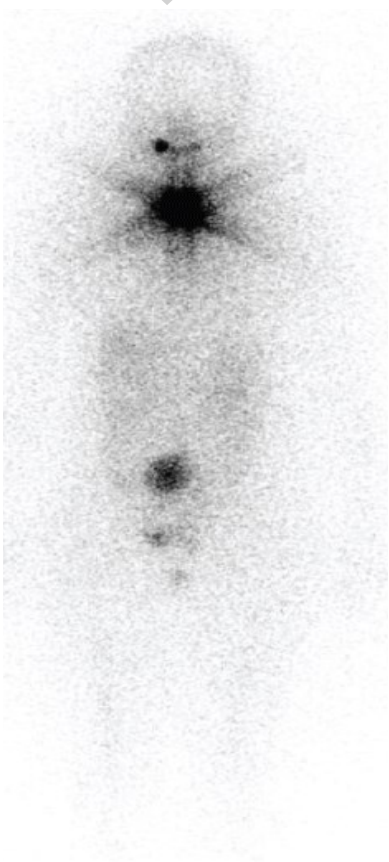

Contents:

STR – 0027 I P.D. SEP 2020

Levothyroxine sodium

Eltroxin

50 mcg and 100 mcg tablet

Thyroid Hormone[1]

Thiamazole

Strumazol®

10mg & 30mg Tablet

Sulfur-Containing Imidazole Derivative[2]

References:

1. Eltroxin Product Insert
2. Strumazol Product Insert

aspen PHILIPPINES

Healthcare. We Care.

Unit 1001-1002, 10th Floor
Trade and Financial Tower
7th Avenue cor. 32nd Street
Bonifacio Global City, Taguig City

Thyroid Health

Philippine Journal of Nuclear Medicine

Volume 16 No. 2
July to December 2021

Official Publication of the Philippine Society of Nuclear Medicine

The Philippine Journal of Nuclear Medicine is a peer-reviewed journal published by the Philippine Society of Nuclear Medicine. Subscription is free to all PSNM members in good standing as part of their membership privileges.

The Journal will be primarily of interest to medical and paramedical personnel working in nuclear medicine and related fields. Original works in clinical nuclear medicine and allied disciplines in physics, dosimetry, radiation biology, computer science, radiopharmacy, and radiochemistry are welcome. Review articles are usually solicited and published together with related reviews. Case reports of outstanding interest are likewise welcome. PSNM documents and position papers of interest to the reader will also be published as necessary.

Manuscripts for consideration should be sent to:

The Editor, Vincent Peter C. Magboo, MD
Philippine Journal of Nuclear Medicine
c/o Philippine Society of Nuclear Medicine
Unit 209 One Beatriz Tower Condo
4 Lauan St. cor. Aurora Blvd
Project 3, Quezon City 1102, Philippines
Contact. No.: +63 (966) 976 5676
Email: vcmagboo@up.edu.ph
philnucmed@gmail.com

All business communications and requests for complimentary copies should be addressed to the above.

ISSN 1655-9266

INFORMATION FOR AUTHORS

EDITORIAL POLICY

The Philippine Journal of Nuclear Medicine is the official peer-reviewed publication of the Philippine Society of Nuclear Medicine. The Journal accepts original articles pertinent to the field of nuclear medicine. Articles may be on any of the following: clinical and basic sciences, case reports, technical notes, special contributions, and editorials.

Submission of manuscripts

The submitted manuscript package should consist of: (1) the full text (including tables) in Microsoft Word, plain text or ConTeXt document format; and (2) high-resolution JPEG files of all images used in the manuscript. The complete manuscript package may be submitted as a compressed (.ZIP) file by email to philnucmed@gmail.com, or in an optical disc (CD/DVD) and mailed to

> The Editor: Philippine Journal of Nuclear Medicine, c/o Philippine Society of Nuclear Medicine, Unit 209 One Beatriz Tower Condo, 4 Lauan St. cor. Aurora Blvd., Project 3, Quezon City 1102, Philippines.

Manuscripts should be accompanied by a cover letter signed by the author responsible for correspondence regarding the manuscript. The cover letter should contain the following statement:

"All copyright ownership is transferred to the Philippine Journal of Nuclear Medicine upon acceptance of the article _____. This manuscript has been seen and approved by all the authors. The authors stipulate that the material submitted to the Philippine Journal of Nuclear Medicine is an original work and has not been submitted to another publication for concurrent consideration. Any human and/or animal studies undertaken as part of the research are in compliance with regulations of our in stitution(s) and with generally accepted guidelines governing such work."

The cover letter should also give any additional information that may be helpful to the Editor. Signed cover letters sent by email should be in PDF format.

MANUSCRIPT FORMAT

Manuscripts must be written in English, and printed on letter-sized white bond paper, 8.5 in x 11 in (21.6 cm x 27.9 cm). The text should be on one side of the paper only, single-spaced, with at least 1.5 in (4 cm) margins on all sides. Each of the following sections must begin on separate pages and in the following order: title page, abstract, text, acknowledgments, references, tables (each on a separate page), and legends. Pages should be consecutively numbered beginning with the title page. The first line of paragraphs should be indented by at least five spaces.

Title page

The title page should include: (1) a concise but informative title; (2) a short running head or footline of no more than 40 characters; (3) a complete byline, with first name, middle initial, and last name of each author and highest adacemic degrees; (4) the complete affiliation for each author, with the name of departments and institutions to which the work should be attributed; (5) disclaimers, if any; (6) the name, address, and telephone number of the author responsible for correspondence about the manuscript; and (7) the name and address of author to whom reprint requests should be directed.

Abstract and key words
An abstract of no more than 300 words should state the purpose of the study or investigation, summary of methodology, major findings, and principal conclusions. New and important aspects of the study or observations should be emphasized. No figures, abbreviations or reference citations are to be used in the abstract.

Text

The text of original scientific and technical articles is usually divided into the following sections: Introduction, Materials and Methods, Results, Discussion, and Summary or Conclusion.

Case reports are divided into the following sections: Introduction, Case Report, Discussion, and Conclusion. They should contain a concise description of one to three patients, emphasizing the nuclear medicine aspects and include methodology, data and correlative studies. Procedures should be described in sufficient detail to allow other investigators to reproduce the results.

Other articles, e.g. review articles, position papers, or editorials, should introduce a problem or question, present evidence, and conclude with an answer. Generally, review articles should have extensive documentation. Literature citations should represent the breadth and depth of the subjects being reviewed. The organization of review articles will depend greatly on the subject matter and material.

Generic names must be used throughout the text. Instruments and radiopharmaceuticals must be identified by manufacturer name and address in parentheses.

Acknowledgments

Persons or agencies contributing substantially to the work, including any grant support, must be acknowledged.

References

References must be cited in consecutive numerical order at first mention in the text and designated by the reference number in parentheses. References appearing in a table or figure should be numbered sequentially with those in the text.

The reference list must be numbered consecutively as in the text. The journal follows Index Medicus style for references and abbreviates journal names according to the List of Journals Indexed in Index Medicus. 'Unpublished observations' and 'personal communications' should not be used as references, although written—not verbal—communications may be noted as such in the text. The author is responsible for the accuracy of all references and must verify them against the original document.

For journal articles with six or less authors, all authors must be listed. For those with seven or more authors, only the first three are listed, and "et al." is added to the end of the list.

> Seabold JE, Conrad GR, Kimball DA, Ponto JA and Cricker JA. Pitfalls in establishing the diagnosis of deep venous thrombophlebitis by indium-111 platelet scintigraphy. J Nucl Med 1988;29:1169–1180.

For book and book chapters:

> Williams LJ. Evaluation of parathyroid function. In: Brock LJ, Stein JB, eds. The parathyroid and its diseases. 4th ed. New York: Wiley; 1985:196–248.
>
> Goodyear B. Bone marrow transplantation in severe combined immunodeficiency syndrome. In: Gree HJ, Blackscmith R, eds. Proceedings of the fourth biennial meeting of the International Society of Transplantation. Houston: International Society of Transplantation; 174: 44–46.

For journal article in electronic format:

> Author. Title. Journal name. Online publishing date. Available from: URL address.

Tables

Each table should be typed double-spaced on a separate page. Do not submit tables as photographs. Tables should be self-explanatory and should supplement, not duplicate, the text. Each table must be cited in consecutive numerical order in the text. Tables should be numbered consecutively with a Roman number following the word TABLE.

Illustrations

Illustrations should clarify and augment the text. Figures should be sharp and of high quality. Glossy photographs of line drawings rendered professionally on white drawing paper in black India ink, with template or typeset lettering, should be submitted. High quality computer-generated art is also acceptable. Letters, numbers, and symbols should be clear and of sufficient size to retain legibility after reduction.

Each illustration must be numbered and cited in consecutive order in the text. Illustrations should be identified on a gummed label. Legends should be typed double-spaced on a separate page. Figures should be numbered with an Arabic number following the word FIGURE.

Units of measurement

Use of the International System of Units (SI) is standard. Measurements of length, height, weight, and volume must be reported in metric units. Other measurements must be reported in the units in which they were made. Alternative units (non-SI units) should be added in parentheses by the author, if indicated.

Abbreviations and symbols

Only standard abbreviations and symbols should be used in the text. At first mention, the complete term, followed by its abbreviations in parentheses, must be used in the text. Standard units of measure should not be expanded at first mention. Consult a style manual, if necessary.

REVIEW PROCEDURE

Submitted manuscripts are peer-reviewed for originality, significance, adequacy of documentation, reader interest, composition, and adherence to the guidelines. Manuscripts are returned to the author for revision if suggestions and criticisms have been made. All accepted manuscripts are subject to editing for scientific accuracy, clarity, and style.

Med Choice™

Endocrine

Better choice. Better lives.

SA HYPOTHYROIDISM

May Choice Ka!

Med Choice™

Endocrine

Better choice. Better lives.

SA HYPERTHYROIDISM May Choice Ka!

Message from the President of the Society

Dear Colleagues and Friends,

Mabuhay!

It is with great pride and honor to write a message in the January-July 2021 issue of the Philippine Journal of Nuclear Medicine.

In the past two years, we experienced unprecedented circumstances brought about by the Covid-19 pandemic. Nuclear Medicine services in some institutions came to a halt due to difficulty in transporting isotopes and to give way to the more essential services. The PSNM remains grateful and salute the efforts made by all our colleagues, associates and members who stood their ground and have kept the light scintillating during these dark moments. We also remember and pray for our dear friends who we lost in this pandemic some of whom played major roles in the current existence of the PJNM, namely Drs. Gerard Fabian Goco, Joel Mendoza and Blesilda Pono.

PSNM will be turning 56 in 2022, we, the board members are humbled to be elected to lead our society with energy and dynamism while adjusting to the new normal. In recent years we have seen the continuous expansion of the Nuclear Medicine community in the Philippines as evidenced by the establishment of new Nuclear Medicine centers in different parts of the country. While the pandemic poses a challenge, we will do our best in aligning our strategies to keep up with this growth as we remain hopeful in future developments within the Nuclear Medicine community. The PSNM will also continue to strengthen its relationship and collaboration with international organizations such as the IAEA, EANM, WARMTH, AOFNMC, ASNM and WFNMB.

Globally, we have witnessed the unraveling of new discoveries and developments in Nuclear Medicine in the era of precision and evidence-based medicine. Advancements in Molecular Imaging and Theranostics have kept our colleagues optimistic and excited for the future of Nuclear Medicine. As our former editor in chief, Dr. Jerry Obaldo wrote in the 2003 issue of the PJNM, we move a step closer to the creation of the "magic bullet" that we have long dreamt of. The PSNM will continue to provide continuing medical education to keep up with these changes and we commend our scientific committee for coming up with a comprehensive scientific program and for inviting distinguished speakers in this year's 37th PSNM Annual Convention with the theme Updates and Refresh having incorporated basic Nuclear Medicine concepts and the aforesaid new technologies and methodologies.

We also wish our editor in chief Dr. Vincent Peter Magboo and his editorial staff the very best and thank them for their continued efforts in maintaining and improving the quality of our journal. PSNM recognizes the importance of research as it promotes critical thinking, arouses intellectual curiosity, and will help improve the quality of the practice of our specialty. We, therefore, encourage our members and trainees to indulge in cutting-edge research and methodologies and appeal to our training institutions to send their quality work for publication.

Lastly, we are looking ahead with great optimism of becoming a better and stronger society in the next decade and we are kindly requesting for your continued kind support and participation.

Thank you very much!

Warmest regards,

Francis Gerard M. Estrada, MD, FPSNM

President, Philippine Society of Nuclear Medicine (2021-2023)

Message from the Editor

Greetings from your Editor!

COVID-19 has affected the practice of nuclear medicine practice significantly not only locally but globally. This pandemic has imposed significant challenges on our local health-care systems leading to reduced services for both in-patient and outpatient for all diseases. Stringent infection prevention and control measures become standard and common in all health institutions. COVID-19 indeed truly changed the way we do things in relation to constraints in the organization, clinical, imaging and research activities in nuclear medicine. This has affected our clinical practice and our interaction with patients and colleagues.

Despite all these, research activities should adhere to the notion of "the show must go on" as a semblance of return to normalcy and continuity of healthcare services to our patients. We believe that research activities in nuclear medicine should not end due to the COVID pandemic. In fact, many studies have already been published to determine and assess extent of pandemic impact to our practice. Worldwide, research agenda have been focused on novel technologies, newer radiopharmaceuticals, and revised methods of imaging paving for exciting and better future in our clinical practice.

As such, it is our responsibility not only to protect and promote the continuity of our innovative scholarly efforts but also do our part to encourage and support the return to normalcy. As a professional society journal, our main goals for the coming years is to encourage more contributions from the nuclear medicine community and to disseminate our findings to the world. We would like to thank our authors, contributors, editors and anonymous reviewers, and readers all of whom have volunteered to contribute to the success of the journal. We are publishing our journal twice a year with a particular emphasis on quality, safety and better outcomes of research.

Thank you very much!

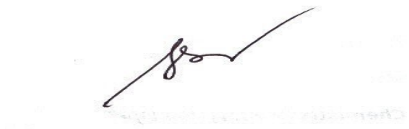

Vincent Peter C. Magboo, MD, FPSNM

Editor, Philippine Journal of Nuclear Medicine

Systematic Review and Meta-analysis comparing the diagnostic utility of Tc-99m tagged RBC scintigraphy with CT-angiography imaging studies in diagnosing Lower Gastrointestinal Bleeding

Jose Carlos T. Chanyungco, MD, Ruben V. Ogbac, MD

Division of Nuclear Medicine, University of the Philippines - Philippine General Hospital
E-mail address: jctc93@gmail.com , rvogbac@gmail.com

ABSTRACT

Background:

Lower Gastrointestinal bleeding (LGIB) is a serious and urgent condition which can be assessed using several different modalities. Tc-99m tagged RBC scintigraphy has been established as a diagnostic tool in Nuclear Medicine but several other modalities, including CT-based imaging (i.e. angiography) currently exist.

Objective:

The objective of this study is to compare Tc-99m tagged RBC scintigraphy with CT-based imaging studies in terms of clinical utility and diagnostic outcomes.

Methods:

A systematic review of available literature was done, with the goal of creating a meta-analysis focusing on the reported diagnostic outcomes - mainly sensitivity and specificity on the presence of a LGIB. Aside from this, a systematic review of the clinical utility and the differences of each test were discussed, including non-quantifiable advantages. The literature search was conducted following the guidelines of PRISMA, with searches from PubMed, Medline, and other pertinent databases. Quality assurance was done using the QUADAS tool. Statistical analyses of sensitivity, specificity, and a summary receiver operating characteristics plot were computed for the meta-analysis.

Results:

Pooled sensitivity and specificity for RBC scintigraphy were 0.886 and 0.119, respectively. Pooled sensitivity and specificity for CT-based imaging were 0.729 and 0.660, respectively. CT based imaging also showed higher localization and faster completion times. RBC scintigraphy had a longer acquisition window.

Conclusion:

Both Tc99m-tagged RBC scintigraphy and CT-based imaging have important clinical utility, with each modality having different advantages that the other test cannot provide.

Keywords*: Tc99m-tagged RBC scintigraphy, red blood cell tagging, gastrointestinal bleed scintigraphy, CT angiography, Multidetector CT, lower gastrointestinal bleed*

INTRODUCTION

Bleeding from the gastrointestinal tract is a serious condition which may lead to mortality in 8-14% of patients [1]. Bleeding within the gastrointestinal tract can be categorized by anatomy. The ligament of Trietz serves as the anatomic demarcation which separates bleeding into upper or lower gastrointestinal in origin. Lower gastrointestinal bleeding (LGIB) usually presents as painless hematochezia, accompanied by a drop in hematocrit values [2]. It accounts for around 20 - 33% of gastrointestinal hemorrhage [3]. According to one study in a tertiary hospital in Manila, LGIB is the most common indication for colonoscopies at around 34% [4].

Several causes of lower gastrointestinal bleeding are possible. According to the UCLA-Center for Ulcer Research and Education (CURE) database [2], the most common etiology is bleeding due to diverticulosis at 30%. This is followed by hemorrhoids and ischemic bowel disease at 14% and 12%, respectively. Management varies depending on the cause of bleeding and patients are usually seen by a multidisciplinary team of clinicians and diagnosticians.

Guidelines from the American College of Gastroenterology as well as the Philippine Society of Digestive Endoscopy recommend several diagnostic tools which a physician may use in evaluating LGIB [5,6].

Gastrointestinal bleeding has long been evaluated using scintigraphy with tagged RBC (also known as the gastrointestinal bleed scan) as one of the less invasive methods of diagnosis. The gastrointestinal bleed scan has proven its sensitivity in detecting a bleed, demonstrating effectiveness even for volumes less than 1 mL. Recently, several CT modalities have been introduced to evaluate GI bleeding. One of which is the CT angiography using a multidetector CT (MDCT). It uses iodinated contrast on the patient and allows for precise localization of any suspected hemorrhage. The CT-angiography imaging modality is currently not recommended as initial work-up for gastrointestinal bleeding, although its use is growing in popularity [7].

Several studies have been published comparing tagged RBC scintigraphy with CT-angiography, with varying results. A meta-analysis of these papers would be useful when considering the role of each modality for the assessment of patients with LGIB.

Objectives:

The primary objective of this study is to review the published literature on Tc-99m tagged RBC scintigraphy and CT-based diagnostics and come out with a conclusion commenting on the comparison between the two. This study also aims to have a set of recommendations for the use of both modalities, but with a focus on GI scintigraphy.

MATERIALS AND METHODS

Search Strategy

A comprehensive review of PubMed and Medline was done using a combination of the following search terms: “red blood cell tagging”, “scintigraphy”, “gastrointestinal bleed”, “CT angiography”, “Multidetector CT”. A manual review of references within pertinent studies was also done. The complete MeSH terms and search history are attached in the appendix.

Reporting of study results was done following the guidelines of Preferred Reporting Items for Systematic reviews and Meta-Analyses or PRISMA [8]. Two independent reviewers screened for the presence of duplicate results and for proper eligibility based on the title and abstract. The remaining studies were then assessed for eligibility.

Study Selection:

Studies from the initial search were carefully selected by setting several inclusion and exclusion criteria. These criteria were made to best answer the objectives of this paper.

The following are the inclusion criteria for the studies:

1. Studies must deal with patients who were worked up for acute lower gastrointestinal hemorrhage
2. Studies must have a direct comparison between RBC scintigraphy and CT-based imaging
3. Studies must report on either the clinical utility of each modality or at least one of the following diagnostic outcomes: sensitivity, specificity, localization
4. Studies must have actual patient populations who undergo each diagnostic test.

Below are the exclusion criteria for the studies:

1. Studies must not be a case-series, case report or a cohort study comparing different disease stages of LGIB.
2. Studies with less than 15 total patients will not be included
3. Studies must not be published earlier than 2005

Only the studies which fulfilled all of the inclusion criteria below were considered. Studies dealing with upper gastrointestinal hemorrhage were not in the inclusion criteria since RBC-tagging is not a usual diagnostic tool used for evaluation. In addition, studies that only examined one modality while just referencing the other modality were also not considered to avoid possible sources of bias.

Studies which possessed all the inclusion criteria were further filtered by the exclusion criteria. Cohort studies with diagnostics done at different disease stages were excluded in order to avoid testing for the presence of hemorrhage at different periods wherein the likelihood of a positive outcome is different. If the modalities were used at different time periods, an unacceptable amount of bias would be included, and this would disregard the evolution of the disease over time. An example of a study that would have been excluded was one where a certain modality was used as the initial work-up and the other modality used for a different purpose such as assessing efficacy of an intervention.

Case-series and case report studies were excluded since the designs of these studies cannot predict sensitivity and specificity based on the limited sample size

Study Quality Assessment and Data Extraction

Eligible studies were evaluated for their quality using the Quality Assessment of Diagnostic Accuracy Studies 2 (QUADAS-2) tool to assess for bias and applicability. The QUADAS-2 tool was made to assess four pertinent aspects of a diagnostic study, which are: 1) patient selection, 2) index test, 3) reference standard and, 4) flow and timing [9]. The highest score a study can have is 14, with the lowest possible score of 0. Studies that scored 7 or less were not included in the review.

The specificity and sensitivity of each modality in diagnosing the presence of LGIB was extracted from the reported raw data and was also recomputed by the investigator. Separately, the rate of accurate localization was also extracted and the number of patients who were part of the study was also noted.

A study was considered positive if it was able to correctly identify the presence of bleeding, regardless of the findings on its localization. Only data from index tests which had a corresponding reference standard were included for the computation in the meta-analysis. However, studies which did not use an acceptable reference standard were still noted for the discussion. Clinical utility and other differences between the modalities which could not be statistically analyzed were also accounted for in the systematic review. Two independent reviewers discussed their respective assessments with a third reviewer available to resolve differences via consensus.

Statistical Analysis

A meta-analysis of studies which report the same clinical outcomes was done while studies which do not qualify for the meta-analysis were included in the discussion of the review. Data from the index tests, namely RBC scintigraphy and CT-based imaging, were extracted from each study. If available, this would be compared to the reference standard, which was catheter/conventional angiography. Also, surgical confirmation was also accepted as a reference standard. Sensitivity and specificity were recomputed for each study based on their presented raw data. Useable data was disaggregated from studies which only reported overall outcomes. Particularly, data disaggregation was done to separate the index tests that were evaluated against a reference standard from the index tests without proper comparison. Pooled sensitivity and specificity were then computed based on the extracted data. Accurate localization of a positive study was also extracted if available. Heterogeneity of the studies were analyzed during the pooling of sensitivity and specificity

To address the variabilities between the chosen studies, a summary receiver operating characteristic (SROC) curve was used. The SROC curve plots the 1-specificity and the sensitivity in the x- and y-axes using a regression model with a smooth curve as an outcome. From this, the area under the curve (AUC) may be computed with values between zero to one [10]. The AUC value is the probability for which a pair of a true positive and a true negative results is identified properly. An ideal test has an AUC of 1, while a test which randomly and equally assigns positive and negative results has an AUC of 0.5. The SROC analysis considers the different thresholds of positivity used in each study and the differences in population number, both of which are pitfalls when using pooled sensitivity, specificity, and averages [10]. The SROC curves and AUC values were generated using the MetaDisc 1.4 program.

Data on clinical utility and some other diagnostic outcomes were included in the systematic review and discussion, but not included in the SROC curve computation since these parameters can not be fairly compared quantitatively. Examples of these parameters in the discussion include the window period (possible acquisition time) for which bleeding can be seen.

RESULTS

Literature Search Outcome

A total of 182 studies were initially screened for eligibility based on the aforementioned search terms and combinations. Majority of the studies were excluded because they tackled a different subject matter. Six studies were deemed eligible to be included in the systematic review, based on the inclusion and exclusion criteria. However, two of the studies were not included in the meta-analysis due to differences in design and reported outcomes. The four studies included in the meta-analysis amounted to a total number of 374 patients. The diagram of the search flow following PRISMA is in the appendix. The list of the studies, alphabetically arranged by authors, may be seen in Table

1. Table 1 also indicates the study design and comments on how data was reported or used.

Characteristics of the studies

Among the selected studies, three (the studies by Awais, Kulkarni and Speir) compared the diagnostic outcomes of both index modalities using catheter angiography as the reference standard. All three were retrospective reviews of patients who underwent a catheter angiography (the reference standard) and had a CT-angiography and/or RBC scintigraphy. The study by Zink was a prospective evaluation of CT-angiography compared with RBC scintigraphy, however, not all patients were subject to catheter angiography or surgery. For this study, data was disaggregated and only the portion of the population which had an acceptable reference standard comparison was included in the meta-analysis.

Table 2 shows the total patient population and the number of procedures done for each index test for each study. Some patients underwent both tagged-RBC scintigraphy and CT-angiography, while other patients underwent work-up twice. The study by Kulkarni retrospectively looked at all patients who underwent CT-angiography, thus the entire population had the test done. The studies by Awais and Speir retrospectively went through all patients who were worked-up for LGIB, regardless of work-up done.

The study by Hsu only reported on the time for index test completion and time from the index test to catheter angiography. These diagnostic outcomes were not included in the meta-analysis by the investigator but included in the discussion. Data on the outcomes of the catheter angiography were not reported, thus sensitivity and specificity were not available. The study by Feuerstein reported diagnostic outcomes between both modalities, however the index tests served as its own reference standard, making the data on sensitivity and specificity incomparable with the other studies in the meta-analysis. However, Feuerstein also reported on the time for test completion, similar to the study by Hsu, thus making this portion of the study eligible for comparison in the systematic review.

TABLE 1. List of studies, alphabetically arranged by author, with study design and comments on their use in the paper

Study Title	Author and Year	Study Design	Comments
Accuracy of 99mTechnetium-labeled RBC Scintigraphy and MDCT With Gastrointestinal Bleed Protocol for Detection and Localization of Source of Acute Lower Gastrointestinal Bleeding	Muhammad Awais, MBBS et al (2015)	Retrospective	Included in meta-analysis
Localizing Acute Lower Gastrointestinal Hemorrhage: CT Angiography Versus Tagged RBC Scintigraphy	Joseph D. Feuerstein, et al (2015)	Retrospective	Used the index test as its own reference standard
Time to conventional angiography in gastrointestinal bleeding: CT angiography compared to tagged RBC scan	Michael J. Hsu, et al (2019)	Retrospective	Only reported on time
In the workup of patients with obscure gastrointestinal bleed, does 64-slice MDCT have a role?	Chinmay Kulkarni, et al (2012)	Retrospective	Included in meta-analysis
Correlation of CT Angiography and 99m Technetium - Labeled Red Blood Cell Scintigraphy to Catheter Angiography for Lower Gastrointestinal Bleeding: A Single -Institution Experience	Ethan J. Speir, et al (2019)	Retrospective	Included in meta-analysis
Noninvasive Evaluation of Active Lower Gastrointestinal Bleeding: Comparison Between Contrast- Enhanced MDCT and 99mTc-Labeled RBC Scintigraphy	Stephen I. Zink, et al (2008)	Prospective	Disaggregated data was included in meta-analysis

TABLE 2. Patient population and number of procedures for each index test done

	Total patient population	Number of RBC scintigraphy studies	Number of CT-angiography studies
Awais	76	56	25
Kulkarni	50	11	50
Speir	207	185	50
Zink	41	22*	22*
Total number	**374**	**274**	**147**

*Disaggregated data was used. The reported numbers are those wherein both the index test and the reference study were done.

The acquisition protocol of all modalities were reviewed. In all six studies, the tagged-RBC scintigraphy was performed using doses ranging from 555 MBq to 925 MBq of radiopharmaceutical. The RBCs were tagged with Tc-99m pertechnetate using the in-vitro technique. All acquisitions were made via planar imaging and none of the studies performed SPECT-CT fusion imaging. For the CT-angiography test, imaging using intravenous iodinated contrast at 300 mg I/mL was done in the arterial phase, with variable amounts of contrast used in each study. All studies used at least a 64-slice CT. Acquisition of the arterial phase was timed differently for each study, either after a few seconds after bolus or once the 150 HU-enhancement threshold was reached. Contrast-enhanced images were compared with non-contrast images taken prior. Each study followed the acceptable protocol for all modalities for their institution and all images were reviewed by experienced radiologists.

Quality of Selected studies

The selected studies were of moderate to good quality. Two studies scored twelve in the 14-point QUADAS tool for assessment of bias, while there was one study each scoring 11, 10, and 9 points. The study by Hsu, which only reported on completion times, scored 13 points. A detailed breakdown of the QUADAS scoring is in the appendix. These scores show that the studies selected had possible sources of bias in terms of the design. However, due to the nature of the disease which was being evaluated, as well as the protocols of the index tests and reference standard, the design of the studies were not expected to score full marks.

The studies consistently interpreted the results of the reference standard with prior knowledge of the index test. In some studies, the results of the index test determined clinical action and thus the reference standard was not always performed. Reviewing both tests together was part of the standard of care for patients. Images, from the CT-angiography and nuclear medicine, may easily be retroactively reviewed by investigators but it was difficult to do so with catheter angiography. A fully blinded, prospective, randomized control trial would have theoretically been able to create a better study design, but this would compromise patient care and is unethical. For retrospective studies, blinding was performed wherein the index tests were reviewed without knowledge of the results of the reference standard.

Another common source of potential bias is the ability of the reference standard (catheter angiography) to accurately diagnose the disease entity. This issue shall be further elaborated in the discussion portion of the study.

Results of Statistical Analysis

The results for the sensitivity and specificity values of RBC-tagging and CT-angiography may be seen in Tables 3 to 6. The pooled sensitivity of RBC-tagging is 0.886, higher than that of CT-angiography using MDCT which had a sensitivity of 0.729. Both tests show heterogeneity for sensitivity, although there was considerably less in the analysis of RBC-scintigraphy. Pooled specificity was significantly higher for CT-angiography at 0.660 while the RBC-tagging only had a pooled specificity of 0.119. Both tests for specificity had considerable heterogeneity, with the larger chi-squared value for RBC-tagging specificity attributable to vastly different population numbers. Issues with the reference standard, common to all

TABLE 3. Summary values and confidence intervals for Sensitivity of Tagged-RBC Scintigraphy

Summary Sensitivity: Tagged-RBC Scintigraphy

Study	Sen	[95% Conf. Iterval.]	TP/(TP+FN)	TN/(TN+FP)
Awais	0.813	0.636 - 0.928	26/32	8/24
Kulkarni	0.700	0.348 - 0.933	7/10	1/1
Speir	0.944	0.846 - 0.988	51/54	8/131
Zink	0.944	0.727 - 0.999	17/18	2/3
Pooled Sen	**0.886**	**0.813 - 0.938**		

Heterogeneity chi-squared = 6.91 (d.f.= 3) p = 0.075

TABLE 4. Summary values and confidence intervals for Specificity of Tagged-RBC Scintigraphy

Summary Specificity: Tagged-RBC Scintigraphy

Study	Spe	[95% Conf. Iterval.]	TP/(TP+FN)	TN/(TN+FP)
Awais	0.333	0.156 - 0.553	26/32	8/24
Kulkarni	1.000	0.025 - 1.000	7/10	1/1
Speir	0.061	0.027 - 0.117	51/54	8/131
Zink	0.667	0.094 - 0.992	17/18	2/3
Pooled Spe	**0.119**	**0.074 - 0.180**		

Heterogeneity chi-squared = 21.76 (d.f.= 3) p = 0.000

TABLE 5. Summary values and confidence intervals for Sensitivity of CT-angiography

Summary Sensitivity: CT-angiography

Study	Sen	[95% Conf. Iterval.]	TP/(TP+FN)	TN/(TN+FP)
Awais	0.933	0.681 - 0.998	14/15	10/10
Kulkarni	0.722	0.548 - 0.858	26/36	8/14
Speir	0.852	0.663 - 0.958	23/27	12/23
Zink	0.389	0.173 - 0.643	7/18	3/3
Pooled Sen	**0.729**	**0.629 - 0.815**		

Heterogeneity chi-squared = 15.55 (d.f.= 3) p = 0.001

TABLE 6. Summary values and confidence intervals for Specificity of CT-angiography

Summary Specificity: CT-angiography

Study	Spe	[95% Conf. Iterval.]	TP/(TP+FN)	TN/(TN+FP)
Awais	1.000	0.692 - 1.000	14/15	10/10
Kulkarni	0.571	0.289 - 0.823	26/36	8/14
Speir	0.522	0.306 - 0.732	23/27	12/23
Zink	1.000	0.292 - 1.000	7/18	3/3
Pooled Spe	**0.660**	**0.512 - 0.788**		

Heterogeneity chi-squared = 13.14 (d.f.= 3) p = 0.004

studies, will be discussed further in the succeeding section. Aside from this, the low pooled specificity of RBC - tagging was likely skewed by the study of Speir which reported a specificity of 0.061. Individual specificities of 1.00 were also reported by Awais and Zink for CT-angiography and by Kulkarni for RBC-tagging. The presence of all these extreme values may be explained by the small patient pool used by the studies.

As mentioned earlier, an index test which correctly identified the presence of bleeding but incorrectly localized the bleeding site was still considered a positive result when computing for sensitivity and for the SROC curve. The data for correct localization was not present in all studies, thus if the condition of correct localization was applied to one study but not the others, an undue confounding factor will be introduced. This caused the need to separate the analysis on positive/negative diagnosis from the analysis on localization.

The summary receiver operating characteristic (SROC) curves are both seen in Figures 1 and 2, respectively. The area under the curve (AUC) of CT-angiography is higher at 0.81 compared to the 0.77 AUC of RBC-tagging. As seen on the figures, the confidence intervals for the SROC curve at 95% are both large thus this puts into question the clinical relevance of the rather small difference between the AUC of both modalities. As mentioned in the previous section, the SROC analysis takes into consideration the pitfalls of pooled sensitivity and specificity.

The Spearman's correlation coefficient was also derived, with RBC-tagging showing moderate positive correlation at 0.632 and with minimal negative correlation for CT-angiography of -0.2. The p-values were both high at 0.368 and 0.8 respectively, thus little clinically useable inferences can be derived.

Accurate localization was demonstrated in all CT-angiography tests from the study of Awais (14 of 14), and with only one (out of 17) misidentified source in the study by Feuerstein. On the other hand, RBC-tagging showed wrong localization in three (out of 26) tests from the study of Awais, in five (out of 34) from the study of Feuerstein, and one (out of 17) from the study of Zink. The remainder of the studies did not report on localization results. Further statistical analysis of the data was not done since there were inconsistencies between the studies on how localization was determined, however, the individual data sets showed that CT-angiography outperformed RBC-tagging.

Time from study order to completion showed a significantly faster completion time of CT-angiography on both studies which reported on it. The study by Hsu reported an average time to completion of 3 hours and 4 minutes for CT-angiography compared to 5 hours and 1 minute for RBC-tagging, while the study by Feuerstein showed an average time to completion of 1 hour and 41 minutes for CT angiography compared to 3 hours and 9 minutes for RBC-tagging. Significant differences between the averages of the same index

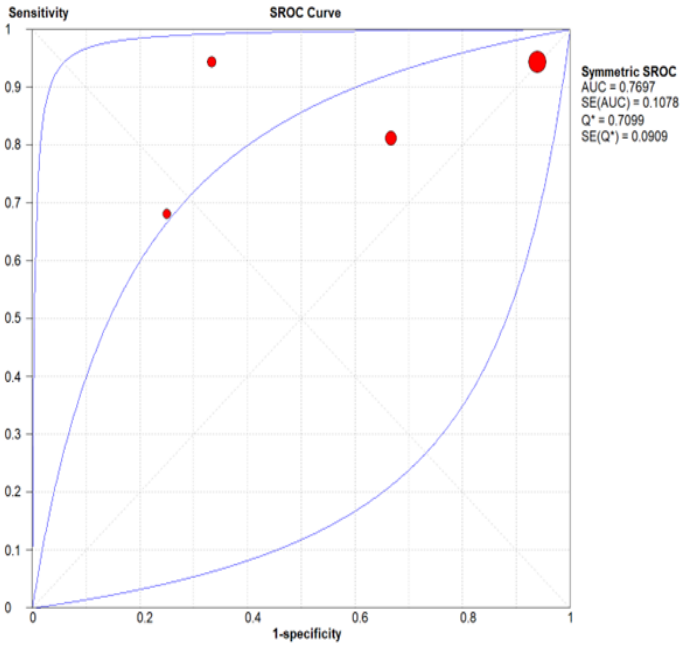

FIGURE 1. SROC curve for RBC-tagging scintigraphy

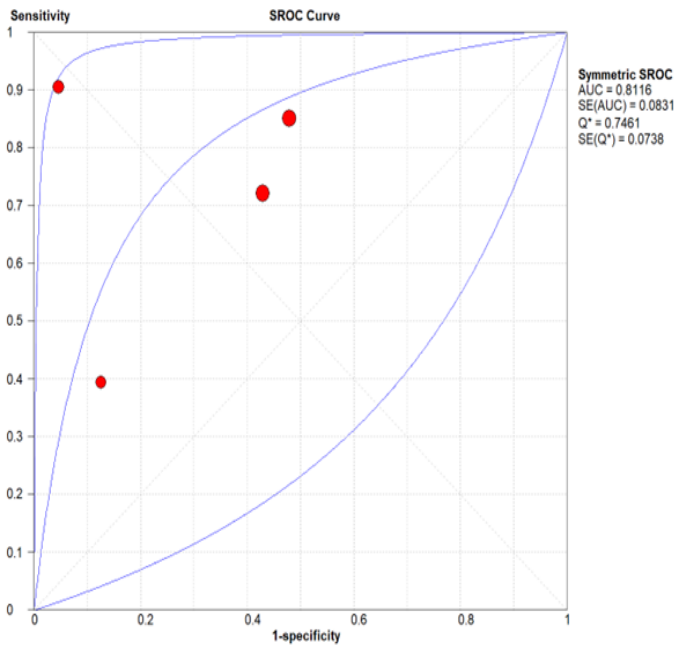

FIGURE 2. SROC curve for CT-angiography

test from the two studies may be attributed to the inter-hospital differences. A larger window for acquisition times for RBC-tagging was present, however, the complete data set was not reported in both studies.

DISCUSSION

Assessment and comparison of the two index tests is complex and should be done with careful discussion of the inherent differences each modality has. The AUC values of CT-angiography and tagged RBC scintigraphy were too close to be significant given the large confidence intervals. This implies the same likelihood that the two index tests will classify a pair of true positive and negative correctly. A number of the included studies discussed and concluded that CT-angiography demonstrates greater accuracy based on their sensitivity and specificity [13, 15], while others were not able to definitively conclude that there was statistically significant disagreement [17]. However, all studies agreed that both modalities were useful in evaluation of LGIB. Although different protocols for the sequence of which imaging modality for LGIB were used in the included institutions, a positive or negative finding in either of the index tests affected the management of the patient and both were clinically useful, regardless.

The derived sensitivity and specificities from the selected studies for RBC-tagging scintigraphy was lower than what is usually reported in other sources of literature. A sensitivity of higher than 90% is usually the accepted value with greater variance in the reported specificities, ranging from 30% to 90% [17]. Gastrointestinal bleeding as low as 0.1 mL/min can be detected by scintigraphy, with an imaging window of up to 24 hours from injection of the radiopharmaceutical [17, 23, 24] The small amount of bleeding needed as well as the large window of imaging contributes to the high reported sensitivity of scintigraphy in literature, with some even reporting values nearing 100% of active bleeding [20]. The pooled sensitivity at 0.866 may have been improved if a more thorough imaging protocol was done. Majority of the studies did not mention if delayed images were taken, considering the fact that the time of study order to completion only averaged at 5 hours in one study [15] and 3 hours in another [16].

The pooled specificity of RBC scintigraphy derived from the studies was 0.119, which is lower than what is reported in literature [17]. A possible explanation for this may come from the formula of specificity which is (true negatives) / (true negatives + false positives), focusing on the false positives. A study was deemed to be falsely positive if the index test (RBC-tagging scintigraphy) reported a positive result while the reference standard (catheter angiography) showed a negative result. Catheter angiography involves insertion of a catheter that delivers contrast which will extravasate into the gastrointestinal tract in the presence of active bleeding. This is the confirmatory sign of bleeding. Aside from this diagnostic utility, therapeutic embolization may also be done concurrently, making this a first-line imaging modality in gastrointestinal bleeding for some cases [18].

Despite being a reference standard, it is not uncommon that there are cases wherein a patient will test positively in RBC-tagging scintigraphy and negatively in catheter angiography. A 2013 study showed that out of 152 patients who were seen to have bleeding on gastrointestinal bleed scintigraphy, catheter angiography was not able to localize bleeding in 116 or around 76% [18]. The presence of an imperfect gold-standard may cause over- or underestimation of the parameters of the index test. The investigators believe that for majority of the studies, it has incorrectly increased the false positives, thus underestimating specificity. There is little, in terms of data processing, that can be done to rectify the values which come from an imperfect reference standard. A solution that can be offered to assess the presence of an actual condition, gastrointestinal bleeding in this case, is by using multiple tests [19]. In the study by Zink, there were cases where surgical confirmation of bleeding superseded the negative findings of catheter angiography, and thus classifying a patient who tested positive in RBC-scintigraphy as a true positive, despite being negative on catheter angiography [14]. However, only this one study offered data on other means of confirmation and so this method of using multiple tests to augment an imperfect reference standard was not done for all studies.

Similar to the values reported in RBC scintigraphy, CT-angiography also has a higher reported sensitivity and specificity in literature at 85% and 92% compared to the derived values from the included studies at 72.9% and 66% respectively [7]. Unlike gastrointestinal bleed scintigraphy, CT-angiography has a very short window of acquisition of 0.5 seconds [7]. This short acquisition window is likely the cause of a lower sensitivity since it eliminates the possibility of repeat acquisition in order to detect intermittent bleeding. Specificity and bleeding - site localization is also higher due to the inherent advantages of CT-based imaging in determining the anatomy of a patient. Accurate bleeding- site localization

is possible in all patients wherein active extravasation is identified; this was consistent with the findings from two of the studies which reported on site localization [11,16]. In addition, CT-angiography can also reliably identify other sources of bleeding, even if they are not active, such as tumors, AV malformations, or ulcerations [7]. This is a distinct advantage of CT-based imaging over gastrointestinal bleed scintigraphy and was discussed in the studies included in the meta-analysis

An in-depth discussion on tagged-RBC scintigraphy done with SPECT-CT acquisition was not present in all studies. Fused imaging of functional images from SPECT with anatomic imaging from CT drastically increased the ability to localize the source of bleeding. Studies show varying degrees of increased localization, with accuracy being 10-15% and up to 36% better than planar imaging [20, 21]. Addition of SPECT-CT fusion imaging does not compromise acquisition of planar imaging while offering the advantages of CT anatomic imaging [23]. The sensitivity in detecting a gastrointestinal bleed may still remain the same even with SPECT-CT fusion since interpretation of a positive scan still hinges on the interpretative criteria from scintigraphy [23, 24]. Comparing SPECT-CT gastrointestinal bleed scintigraphy with CT-angiography may be an interesting avenue to explore since no such paper was identified in the literature search.

The investigators believe that each patient must be evaluated individually with specific clinical scenarios calling for one index test over another. An example of this is RBC-tagging having distinct advantages for occult or intermittent bleeding while CT-angiography is better for localization with relatively larger bleeding volumes. The American College of Radiology (ACR) has released appropriate use criteria for both index tests, which can help guide the clinician as to when a test is appropriate [22]. Briefly, the ACR recommended both RBC scintigraphy and CT-angiography in a hemodynamically stable patient with active bleeding, meanwhile it only recommended CT-angiography in an unstable or transfusion-requiring patient.

CONCLUSION

To summarize, both tagged RBC scintigraphy and CT-angiography are clinically relevant and accurate tests to evaluate lower gastrointestinal bleeding. Sensitivity and AUC values derived from the SROC curves are comparable between both studies with tagged RBC scintigraphy showing a slight but not statistically significant advantage in sensitivity. CT-angiography showed greater specificity but issues with the reference standard likely compounded the results for tagged RBC scintigraphy causing lower values. Both index tests showed distinct advantages over the other such as a large window for acquisition for scintigraphy and accurate anatomic localization for CT angiography.

Limitations of the Study and Recommendations :

This paper is limited by the small number of studies which qualified given the inclusion and exclusion criteria. Furthermore, different methodologies between studies made direct comparison quite difficult. The small population for each individual study lessens the statistical significance which was inferred, as seen by the wide confidence intervals in the SROC.

Recommendations for further studies include reassessment of catheter angiography as a reference standard for other diagnostic modalities. More individual studies are also needed to create a robust data set where more definitive conclusions can be made. The roles of CT-angiography and tagged-RBC scintigraphy should be continuously reassessed when managing LGIB. The addition of SPECT-CT to tagged-RBC scintigraphy may be an interesting avenue to explore, given the added advantages it may give and lack of current literature.

REFERENCES

1. Yoon W., et al (2006) Acute Massive Gastrointestinal Bleeding: Detection and Localization with Arterial Phase Multi-Detector Row Helical CT. Radiology, 239(1), https://doi.org/10.1148/radiol.2383050175 .
2. Ghassemi, K. A., & Jensen, D. M. (2013). Lower GI bleeding: epidemiology and management. Current gastroenterology reports, 15(7), 333. https://doi.org/10.1007/s11894-013-0333-5 .
3. Vernava AM, Longo WE, Virgo KSA (2010) A nationwide study of the incidence and etiology of lower gastrointestinal bleeding. Am J Gastroenterol. Dec 2010;105(12). :2636-41 2 .
4. Amor, VJ (2006) A Review of the Indications and Diagnostic Yield of Colonoscopy at Manila Doctors Hospital: a 2-Year Retrospective Study, Manila Doctors Hospital .

5. Cabriera MT., et al (2018) Guideline for the Management of Acute Severe Lower GI Bleeding in Adult Patients. Philippine Society of Digestive Endoscopy. Retrieved from: https://www.psde.org.ph/wp-content/uploads/2018/02/PSDE-Guideline-on-the-Management-of-Acute-Severe-LGIB-in-Adult-Patients.pdf .
6. American College of Gastroenterology (2016) ACG Clinical Guideline: Management of Patients With Acute Lower Gastrointestinal Bleeding. American Journal of Gastroenterology. Retrieved from: https://www.spg.pt/wp-content/uploads/2015/07/2-2016-Acute-Lower-GI-Bleeding.pdf) .
7. Wells ML., et al (2018) CT for Evaluation of Acute Gastrointestinal Bleeding. Radiographics 38(4). Retrieved from: https://pubs.rsna.org/doi/10.1148/rg.2018170138#:~:text=CT%20angiography%20is%20an%20accurate,detection%20of%20the%20bleeding%20site .
8. Liberati A, Altman DG, Tetzlaff J, Mulrow C, Gøtzsche PC, et al. (2009) The PRISMA Statement for Reporting Systematic Reviews and Meta-Analyses of Studies That Evaluate Health Care Interventions: Explanation and Elaboration. Ann Intern Med, 151 (4).
9. Whiting PF, Rutjes AW, Westwood ME, et al; QUADAS-2 Group. (2011) QUADAS-2: a revised tool for the quality assessment of diagnostic accuracy studies. Ann Intern Med. 2011 Oct 18;155(8):529-36. doi: 10.7326/0003-4819-155-8-201110180-00009. PMID: 22007046.
10. Jones C., et al (2005) Summary Receiver Operating Characteristic Curve Analysis Techniques in the Evaluation of Diagnostic Tests. Ann Thorac Surg 2005;79:16–20. doi:10.1016/j.athoracsur.2004.09.040.
11. Awais M., et al. (2015). Accuracy of 99mTechnetium-labeled RBC Scintigraphy and MDCT With Gastrointestinal Bleed Protocol for Detection and Localization of Source of Acute Lower Gastrointestinal Bleeding. Journal of Clinical Gastroenterology 2016 Oct;50(9):754-60. doi: 10.1097/MCG.0000000000000462.
12. Kulkarni C., et al. (2012) In the workup of patients with obscure gastrointestinal bleed, does 64-slice MDCT have a role? Indian Journal of Radiology and Imaging February 2012 22 (1). doi: 10.4103/0971-3026.95404.
13. Speir EJ., et al (2019) Correlation of CT Angiography and 99mTechnetium-Labeled Red Blood Cell Scintigraphy to Catheter Angiography for Lower Gastrointestinal Bleeding: A Single-Institution Experience. J Vasc Interv Radiol 2019; 30:1725–1732. https://doi.org/10.1016/j.jvir.2019.04.019.
14. Zink SI., et al (2008) Noninvasive Evaluation of Active Lower Gastrointestinal Bleeding: Comparison Between Contrast-Enhanced MDCT and 99mTc-Labeled RBC Scintigraphy. AJR 2008; 191:1107–1114. doi:10.2214/AJR.07.3642.
15. Hsu MJ., et al (2019) Time to conventional angiography in gastrointestinal bleeding: CT-angiography compared to tagged RBC scan. Abdominal Radiology, 01 Feb 2020, 45(2):307-311. https://doi.org/10.1007/s00261-019-02151-8.
16. Feuerstein JD., et al (2016) Localizing Acute Lower Gastrointestinal Hemorrhage: CT Angiography Versus Tagged RBC Scintigraphy. AJR 2016; 207:578–584. doi: 10.2214/AJR.15.15714
17. Grady E. (2015) Gastrointestinal Bleeding Scintigraphy in the Early 21st Century J Nucl Med February 1, 2016 (57)2, p252-259. Retrieved from: http://jnm.snmjournals.org/content/57/2/252.full.
18. Yi WS., et al (2013) Localization and Definitive Control of Lower Gastrointestinal Bleeding with Angiography and Embolization. The American Surgeon, 2013 Apr;79(4):375-80. PMID: 23574847.
19. Walsh, T., (2018) Fuzzy gold standards: Approaches to handling an imperfect reference standard. Journal of Dentistry, July 2018 74(1) S47-S49. Retrieved from: https://www.sciencedirect.com/science/article/pii/S0300571218301039.
20. Schillaci O, et al (2009): SPECT/CT with a hybrid imaging system in the study of lower gastrointestinal bleeding with technetium-99m red blood cells. Q J Nucl.
21. Otomi Y., et al (2018) The diagnostic ability of SPECT/CT fusion imaging for gastrointestinal bleeding: a retrospective study. BMC Gastroenterol. 2018; 18: 183. PMID: 30526506. Retrieved from: https://www.ncbi.nlm.nih.gov/pmc/articles/PMC6288946/
22. .American College of Radiology (2020) ACR Appropriateness Criteria® Radiologic Management of Lower Gastrointestinal Tract Bleeding. Retrieved from: https://acsearch.acr.org/docs/69457/Narrative/
23. O'Malley JP, Ziessman, & Thrall JH (2021) Nuclear Medicine and Molecular Imaging (5th Ed.) Elsevier, PA.
24. Mettler FA & Guiberteau MJ (2019) Essentials of Nuclear Medicine and Molecular Medicine (7th Ed.) Elsevier, TX .

APPENDICES

Appendix 1. MESH terms and search history

Search Number	Query	Filter	Search Details	Results
3	((scintigraphy) OR (Red Blood Cell tagging)) AND (((MDCT) OR (CT angiography) OR (Multidetector CT) AND gastrointestinal))		(((((("radionuclide imaging"[MeSH Terms] OR ("radionuclide"[All Fields] AND "imaging"[All Fields])) OR "radionuclide imaging"[All Fields]) OR "scintigraphies"[All Fields]) OR "scintigraphy"[All Fields]) OR ((((("erythrocytes"[MeSH Terms] OR "erythrocytes"[All Fields]) OR (("red"[All Fields] AND "blood"[All Fields]) AND "cell"[All Fields])) OR "red blood cell"[All Fields]) AND ("tagged"[All Fields] OR "tagging"[All Fields]))) AND ((((((("multidetector computed tomography"[MeSH Terms] OR (("multidetector"[All Fields] AND "computed"[All Fields]) AND "tomography"[All Fields])) OR "multidetector computed tomography"[All Fields]) OR "mdct"[All Fields]) OR ((((("computed tomography angiography"[MeSH Terms] OR (("computed"[All Fields] AND "tomography"[All Fields]) AND "angiography"[All Fields])) OR "computed tomography angiography"[All Fields]) OR ("ct"[All Fields] AND "angiography"[All Fields])) OR "ct angiography"[All Fields])) OR ((((("multidetector computed tomography"[MeSH Terms] OR (("multidetector"[All Fields] AND "computed"[All Fields]) AND "tomography"[All Fields])) OR "multidetector computed tomography"[All Fields]) OR ("multidetector"[All Fields] AND "ct"[All Fields])) OR "multidetector ct"[All Fields])) AND (("gastrointestinal"[All Fields] OR "gastrointestinally"[All Fields]) OR "gastrointestine"[All Fields]))	174
2	((scintigraphy) OR (Red Blood Cell tagging)) AND (((MDCT) OR (CT angiography)) AND gastrointestinal))		(((((("radionuclide imaging"[MeSH Terms] OR ("radionuclide"[All Fields] AND "imaging"[All Fields])) OR "radionuclide imaging"[All Fields]) OR "scintigraphies"[All Fields]) OR "scintigraphy"[All Fields]) OR ((((("erythrocytes"[MeSH Terms] OR "erythrocytes"[All Fields]) OR (("red"[All Fields] AND "blood"[All Fields]) AND "cell"[All Fields])) OR "red blood cell"[All Fields]) AND ("tagged"[All Fields] OR "tagging"[All Fields]))) AND (((((("multidetector computed tomography"[MeSH Terms] OR (("multidetector"[All Fields] AND "computed"[All Fields]) AND "tomography"[All Fields])) OR "multidetector computed tomography"[All Fields]) OR "mdct"[All Fields]) OR ((((("computed tomography angiography"[MeSH Terms] OR (("computed"[All Fields] AND "tomography"[All Fields]) AND "angiography"[All Fields])) OR "computed tomography angiography"[All Fields]) OR ("ct"[All Fields] AND "angiography"[All Fields])) OR "ct angiography"[All Fields])) AND (("gastrointestinal"[All Fields] OR "gastrointestinally"[All Fields]) OR "gastrointestine"[All Fields]))	173
1	((scintigraphy) OR (Red Blood Cell tagging)) AND ((CT angiography) AND gastrointestinal))		(((((("radionuclide imaging"[MeSH Terms] OR ("radionuclide"[All Fields] AND "imaging"[All Fields])) OR "radionuclide imaging"[All Fields]) OR "scintigraphies"[All Fields]) OR "scintigraphy"[All Fields]) OR ((((("erythrocytes"[MeSH Terms] OR "erythrocytes"[All Fields]) OR (("red"[All Fields] AND "blood"[All Fields]) AND "cell"[All Fields])) OR "red blood cell"[All Fields]) AND ("tagged"[All Fields] OR "tagging"[All Fields]))) AND (((((("computed tomography angiography"[MeSH Terms] OR (("computed"[All Fields] AND "tomography"[All Fields]) AND "angiography"[All Fields])) OR "computed tomography angiography"[All Fields]) OR ("ct"[All Fields] AND "angiography"[All Fields])) OR "ct angiography"[All Fields]) AND (("gastrointestinal"[All Fields] OR "gastrointestinally"[All Fields]) OR "gastrointestine"[All Fields]))	158

Appendix 2. PRISMA Diagram

QUADAS						
	Zink	**Feuerstein**	**Kulkarni**	**Speir**	**Awais**	**Hsu**
Was the spectrum of patients representative of the patients who will receive the test in practice?	Yes	Yes	Yes	Yes	Yes	Yes
Were selection criteria clearly described?	Yes	Yes	Yes	Yes	Yes	Yes
Is the reference standard likely to correctly classify the target condition?	No	No	Yes	No	No	N/A
Is the time period between reference standard and index test short enough to be reasonably sure that the target condition did not change between the two tests?	Yes	Yes	Yes	Yes	Yes	Yes
Did the whole sample or a random selection of the sample, receive verification using a reference standard of diagnosis?	No	No	No	Yes	Yes	Yes
Did patients receive the same reference standard regardless of the index test result?	No	No	No	Yes	Yes	Yes
Was the reference standard independent of the index test (i.e., the index test did not form part of the reference standard)?	Yes	No	Yes	Yes	Yes	Yes
Was the execution of the index test described in sufficient detail to permit replication of the test?	Yes	Yes	Yes	Yes	Yes	Yes
Was the execution of the reference standard described in sufficient detail to permit its replication?	Yes	Yes	Yes	Yes	Yes	Yes
Were the index test results interpreted without knowledge of the results of the reference standard?	Yes	Yes	Yes	Yes	Yes	Yes
Were the reference standard results interpreted without knowledge of the results of the index test?	No	No	No	No	No	Yes
Were the same clinical data available when test results were interpreted as would be available when the test is used in practice?	Yes	Yes	Yes	Yes	Yes	Yes
Were uninterpretable/ intermediate test results reported?	Yes	Yes	Yes	Yes	Yes	Yes
Were withdrawals from the study explained?	Yes	Yes	Yes	Yes	Yes	Yes
TOTAL	**10**	**9**	**11**	**12**	**12**	**13**

APPENDICES

Appendix 3. PRISMA Diagram

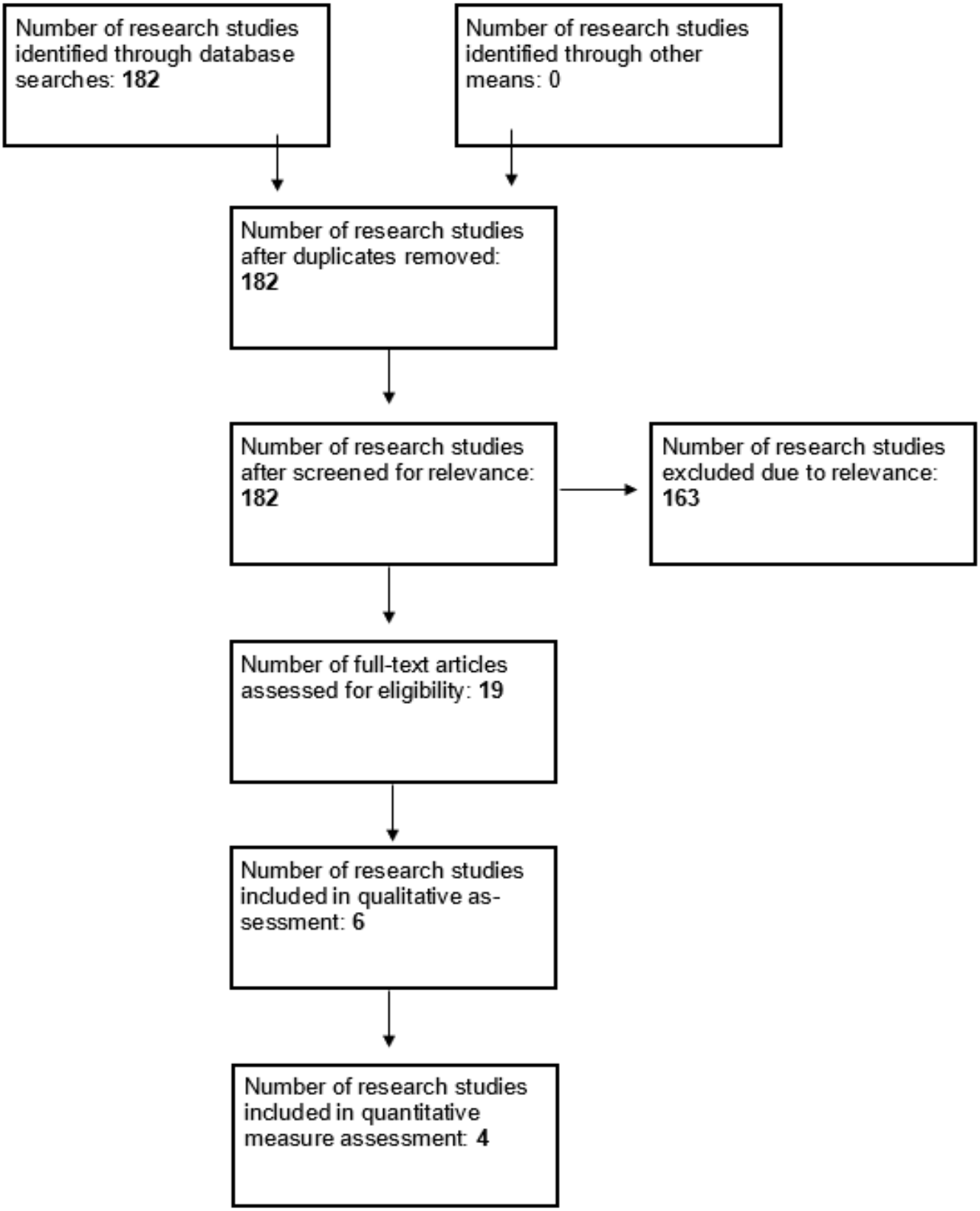

transmedic

advancing medical technologies

NUCLEAR MEDICINE PRODUCT PORTFOLIO

SPECTRUM DYNAMICS MEDICAL

Future-proof Cadmium Zinc Telluride (CZT) based cardiac and nuclear medicine imaging system

D-SPECT CARDIO®

UNITED IMAGING

Ultra-High-Resolution Digital PET/CT with 194 cm Axial FOV

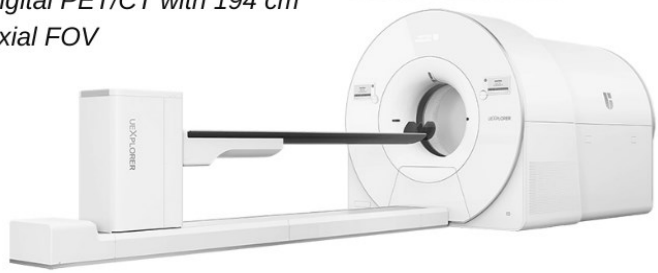

DDD Diagnostic

Gamma Camera for General Purpose Nuclear Medicine

CMR NAVISCAN

Breast-Dedicated Radionuclide Imaging system

Australian Government | ANSTO

Science. Ingenuity. Sustainability.

Sterile Tc-99m Generator

Eckert & Ziegler

Contributing to saving lives

Your one-stop-shop for the complete synthesis: from radionuclides to radiosynthesis and its quality control

BEST ABT MOLECULAR IMAGING

Dose on Demand Biomarker Generator

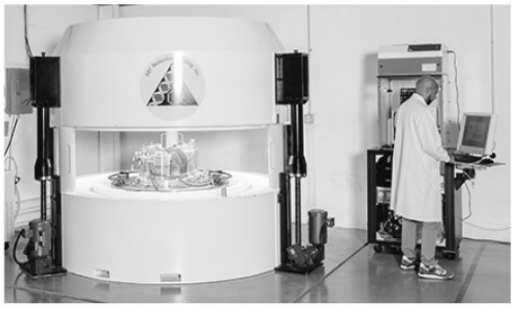

mim Encore

A Comprehensive Solution for PET and Nuclear Medicine

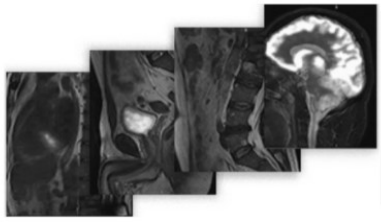

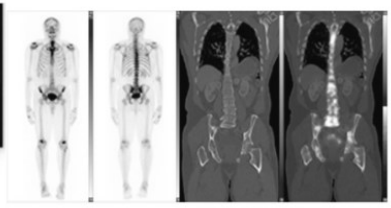

MICROLAB
Since 1966
Committed to Quality Life.

Norland XR-800 Advanced is the top-of-the-line system with a full configuration of scanning applications.

Norland XR-800 Clinical is configured with a strong clinical software package that includes whole body with composition applications.

Norland XR-800 Basic is configured with a basic software package that includes the whole body application.

Norland XR-600 Advanced is the top-of-the-line non-whole body capable system fitted with a broad array of scanning applications.

Norland XR-600 Clinical is configured with a strong clinical non-whole body capable software package applications.

Norland XR-600 Basic is configured with a basic non-whole body capable software package applications.

NORLAND
at Swissray

*ddR*Aura™ OTC APS
Fully automated ceiling suspension

*ddR*Aura™ OTC
Manually positioned ceiling suspension

*ddR*Aura™ Twin leg table

Swissray

INTRODUCING THE 800 SERIES

A True Partnership in True Discovery

A SWIFTER SCAN AND A SMARTER CONSOLE

Diagnose disease earlier with SwiftScan Planar's and SwiftScan SPECT's improved small lesion detectability [1]

Use SmartConsole to create SPECT/CT data sets in PET/CT DICOM format for adjunct review with a PET DICOM viewer

25% REDUCED

Enable reduction of dose or scan times by up to 25 percent with the increased sensitivity of SwiftScan Planar and SwiftScan SPECT [2]

Save time and steps by remotely collaborating with a clinician mid-exam with SmartConsole Web

For more information, please visit **www.gehealthcare.com.sg**

Comparison of Gallium - 68 Prostate-Specific Membrane Antigen (Ga-68 PSMA) Normal Tissue Uptake across Tumor Burden Groups among Filipino Patients with Prostate Cancer

Mary Stephanie Jo C. Estrada, MD, Eduardo Erasto S. Ongkeko, MD, Mia Anne Ryna L. Bayot, RRT, Kalvin B. Catubao, RRT, Klein Reagan R. Bautista, RRT, Patricia A. Bautista - Penalosa, MD

Division of Nuclear Medicine and PET Center, St. Luke's Medical Center - Global City
E-mail address: marystephaniejo2729@gmail.com , eongkekomd@yahoo.com ,miabayot17@yahoo.com , kalvincatubao@gmail.com, bautistaklein26@gmail.com , pattybautista@gmail.com

ABSTRACT

Background:

PSMA-targeted radiopharmaceuticals have been widely studied for their theragnostic role in prostate cancer and were introduced in the Philippines in 2018. The optimal administered activity of ^{177}Lu-PSMA for targeted endoradiotherapy has not yet been established and is thought to be influenced by several factors, including tumor burden. This study investigates the effect of tumor burden on the normal tissue PSMA uptake among Filipino patients with prostate cancer using its diagnostic counterpart, ^{68}Ga-PSMA I&T

Methods:

One hundred four patients imaged with ^{68}Ga-PSMA I&T PET/CT in our institution from January 2018 to May 2020 were included. Patients were visually classified into low, medium, and high tumor burden groups. Maximum and mean standardized uptake values (SUVmax and SUVmean) of the lacrimal glands, parotid glands, submandibular glands, kidneys, liver, spleen, and bone were measured and compared among tumor burden groups.

Results and Conclusions:

^{68}Ga-PSMA I&T uptake in the kidneys, the salivary glands, and the liver, were significantly reduced by approximately 25-50% in patients with high tumor burden. This finding supports the hypothesis that patients with higher tumor load can tolerate higher activity doses of ^{177}Lu-PSMA for endoradiotherapy before developing significant damage to the critical organs. This may serve as a guide towards optimizing and personalizing ^{177}Lu-PSMA I&T administered activity dose for radionuclide therapy.

***Keywords**: Prostate-specific membrane antigen, Ga-68 PSMA I&T, Positron Emission Tomography, PET/CT, bio-distribution, prostate cancer, tumor burden*

INTRODUCTION

Prostate cancer is the second most common cancer among males globally and the third most prevalent in men in the Philippines [1]. Prostate-specific membrane antigen (PSMA) is a cell surface protein overexpressed in most clinically significant prostate cancer cells, up to 1000 times higher than normal prostate [2]. Its expression increases with Gleason score, androgen insensitivity, metastasis, and disease progression [3]. The unique expression of PSMA makes it an excellent marker for detecting prostate cancer recurrence and metastases. In recent years, extensive research has demonstrated excellent diagnostic accuracy of several PSMA-targeted radiotracers for prostate cancer imaging [4], which led to the development of PSMA-labeled radiopharmaceuticals for endoradiotherapy [5]. PSMA labeled with a positron-emitter (Ga-68) is used to image prostate cancer while its counterpart, labeled with a beta-emitting nuclide (Lu-177), is used for targeted radionuclide therapy [6,7]. Ga-68 PSMA I&T (imaging and therapy) is among the most commonly utilized since it is more suited for its theragnostic (the term for therapy plus diagnosis) role with its biodistribution reflective of its ^{177}Lu-labeled counterpart [8]. Lu-177 PSMA radioligand therapy (PRLT) has been shown to be a safe and effective systemic treatment of metastatic castrate - resistant prostate cancer [9,10], but its optimal dose has not yet been established [11]. Despite the term "prostate-specific," lower PSMA accumulation is noted

in several normal organs such as the lacrimal glands, salivary glands, liver, spleen, and kidneys [12]. Clinically, this means that although the expression of PSMA on these cells is significantly lower than prostatic cancer cells, the radiation dose is still delivered to these non-target healthy tissues when ^{177}Lu- PSMA is used for PRLT. The organs identified to be most at risk are the kidneys and salivary glands due to their high physiologic activity [11-13].

In the Philippines, modern theragnostics was first introduced at our institution in January 2018 as it offered ^{68}Ga-PSMA I&T PET/CT and ^{177}Lu-PSMA I&T radioligand therapy (PRLT) services to prostate cancer patients [14]. Targeted endoradiotherapy (i.e., PRLT) aims to provide the maximum radiation dose delivery to the tumor without causing significant radiation-related, non-target healthy tissue damage [15]. This translates to the careful planning of appropriate radionuclide dose for endoradiotherapy. Understanding the factors that may affect tracer biodistribution is necessary to achieve this goal.

One factor that may influence normal tracer biodistribution is the degree of tumor burden. A phenomenon called the tumor sink effect is observed in Nuclear Medicine when high tumor load results in a marked reduction of normal tissue tracer uptake. This occurrence has been reported in several radiotracers used in Nuclear Medicine, such as ^{99m}Tc-methyl diphosphonate (MDP) [16], ^{18}F-fluorodeoxyglucose (FDG) [17] and ^{68}Ga-DOTA-octreotate [18]. On the other hand, there are limited and conflicting data investigating this sink effect using PSMA-targeted radiopharmaceuticals [19-22]. For example, Gaertner et al. concluded that ^{68}Ga-PSMA-11 biodistribution in normal tissues was dependent on tumor load [19], whereas Werner et al. recently reported no sink effect from F-18 DCFPyL [20]. This theory has yet to be extensively investigated with PSMA-targeted radiopharmaceuticals and no data have been recorded in the local setting. This retrospective analysis aims to explore the effect of tumor burden on the ^{68}Ga-PSMA I&T biodistribution in normal tissues among Filipino patients with prostate cancer.

MATERIALS AND METHODS

Patient population

We retrospectively evaluated all patients aged 18 years and older, and histologically or clinically diagnosed with prostate carcinoma who underwent their first ^{68}Ga-PSMA PET/CT at our institution from January 2018 to May 2020. Patients with known renal disease or patients with eGFR <60 during the scan, as well as studies that did not follow proper protocol (i.e., uptake time of >100 minutes and low administered activity of <100 MBq or <2.7 mCi) were excluded from the study. Relevant patient characteristics (age, height, weight, nationality, Gleason score, date of diagnosis, recent PSA value at the time of the scan, and prior interventions), as well as scan-related information (reason for referral, administered activity, and uptake time), were all collected from the institution's database. Body mass index (BMI) and years since initial diagnosis were extrapolated from the given information. This study was approved by the institution's technical and ethical review committees.

Imaging procedure

As part of our institution's standard protocol and in accordance with the joint EANM and SNMMI procedure guideline for prostate cancer imaging version 1.0, ^{68}Ga-PSMA I&T PET/CT scans were acquired approximately 60 minutes after intravenous injection of Ga-68 PSMA I&T and 20 mg furosemide. All PET/CT scans were obtained on a Philips Gemini TF 64 PET/CT scanner. Non-contrast enhanced low-dose CT scan (120 Kv, 50 mAs) was taken, followed by PET imaging in 3D mode at a rate of 2-3 minutes per bed position from skull vertex to toes with patients in supine position. Emission (PET) images were corrected for attenuation based on the low-dose CT data and reconstructed using BLOB-OS-TF (spherically symmetric basis function ordered subset algorithm time of flight). Depending on the clinical situation and referring physician's request, diagnostic CT scans with or without IV contrast were also performed.

Image analysis

PET/CT images were reviewed and analyzed using Philips IntelliSpace Portal (version 10.1, Koninklijke Philips N.V. 2017). Visual classification of tumor burden and uptake quantification were adopted from the Gaertner study [19]. Patients were classified into low, medium, and high tumor burden (TB) groups. Visual classification of the patients' scans was done independently by two experienced Nuclear Medicine physicians. Representative images are shown in Figure 1. Classification of tumor burden was defined as:

1. Low: disease confined to the pelvis or those not classified as high or medium
2. Medium: widespread but faint bone uptake or bone lesions with intense uptake involving less than half of the skeleton (≤ 30 solitary lesions), extensive PSMA - positive lymph node on both sides of the mediastinum, or extensive PSMA-positive lung metastases
3. High: intense disseminated bone uptake (> 30 solitary lesions or diffusely confluent bone lesions involving more than half of the skeleton)

Before the conduct of the study, independent inter-rater reliability (IRR) was done to ensure consistency between the two experts. During the study, the two experts made a careful discussion to resolve discordance.

Tracer uptake was quantified by maximum and mean standard uptake values (SUVmax and SUVmean) based on body weight. For calculation of the SUVs, volumes of interest (VOIs) were drawn as follows: automatic 50% isocontour for lacrimal glands, parotid glands, submandibular glands, and kidneys; spherical 50 mm diameter for liver, 30 mm diameter for spleen, and 25 mm diameter for bone. L3 was preferred for SUV measurement of the bone, but if L3 was seen to have metastasis, then either L4 or L5 was used. Drawing of the VOIs was done independently by three Nuclear Medicine technologists. Mean of measured SUVs was used for final analysis.

Data analysis

Patients were classified into the three independent groups according to tumor burden. Data were statistically analyzed using STATA 14.1. Homogeneity of baseline characteristics was assessed using analysis of variance (ANOVA) and Fisher's exact test with $p \leq 0.05$ for quantitative and qualitative variables, respectively. Tracer uptake SUVmax and SUVmean between patient groups were compared using one-way ANOVA and Kruskal-Wallis H tests, as appropriate. A p-value of ≤ 0.05 was rated as significant. For significant tests, Tukey-Kramer Test and Mann-Whitney U Test were performed as fitting for post-hoc analyses. Normality was tested using the Shapiro-Wilk test. Correlation of SUVs among visual TB, PSA (surrogate TB marker), weight, BMI, administered activity (AA), and uptake time (UT) was evaluated using Spearman and Pearson Correlation Coefficient.

RESULTS

A total of 104 male Filipino patients diagnosed with prostate cancer were included in our analysis. Seventy - six (76) patients were classified in low, 18 in medium, and 10 in high tumor burden groups. IRR for visual classification between the two experts before conducting the study yielded an almost perfect agreement of 90% (27/30).

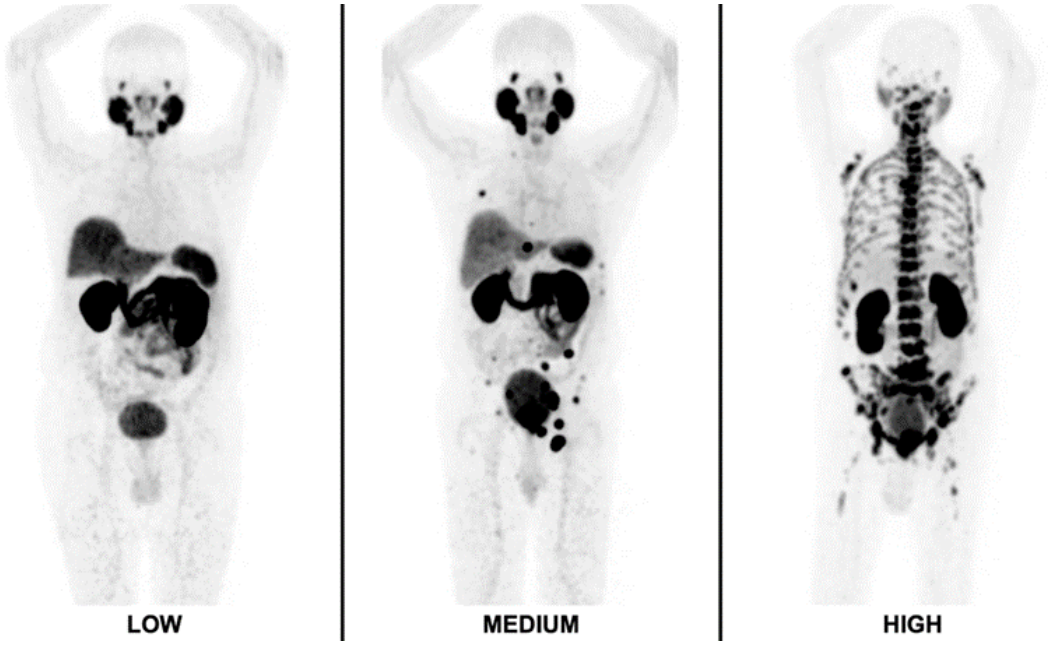

FIGURE 1. Representative maximum intensity projection (MIP) images of Ga-68 PSMA I&T PET/CT visually rated as low, medium, and high tumor burden.

Patient characteristics

The baseline characteristics showed no statistically significant differences among TB groups regarding age, height, weight, BMI, number of years since the initial diagnosis, and Gleason score. Characteristics are summarized in Table 1.

Mean patient age was 69 ± 9 years (range 44-88 years), mean BMI was 26.4 ± 3.5 kg/m2 (range 16.8-33.5 kg/m2) and mean number of years since initial diagnosis was 3 ± 4 (range 0-19 years). A great bulk of the patients were newly diagnosed or referred within the first year of diagnosis (n = 45, 43.3%). Gleason score (GS) was available for only 57 of 104 patients; 47 from the low, 9

TABLE 1. Representative Summary of patients' characteristics

			TUMOR BURDEN			
			Low (n=76)	Medium (n=18)	High (n=10)	p-value
Age (years)		68.7 (9.1)	68 (8.8)	69 (10.2)	72 (9.5)	0.49
Height (cm)		168.2 (6.3)	167.9 (6.4)	169.3 (6.0)	169.2 (6.7)	0.59
Weight (kg)		74.7 (11.3)	74.7 (11.0)	77.7 (10.1)	69.4 (15.1)	0.18
BMI (kg/m^2)		26.4 (3.5)	26.5 (3.4)	27.1 (3.2)	24.2 (4.7)	0.10
Gleason Score		7.6 (1.2)	7.4 (1.1)	8.3 (1.2)	9*	0.06
PSA (ng/mL)		38.11 (90.67)	16.18 (31.14)	41.35 (49.21)	214.34 (224.09)	<0.001
Years since diagnosis		3.0 (4.2)	2.7 (3.9)	3.72 (4.5)	3.8 (5.8)	0.50
Prior surgery	Yes	46 (44.2%)	36 (78.3%)	6 (13%)	4 (8.7%)	0.06
	No	58 (55.8%)	40 (69%)	12 (20.7%)	6 (10.3%)	
Prior chemotherapy	Yes	12 (11.5%)	4 (33.3%)	5 (41.7%)	3 (25%)	0.004
	No	92 (88.5%)	72 (78.3%)	13 (14.1%)	7 (7.6%)	
Prior radiotherapy	Yes	23 (22.1%)	14 (60.9%)	7 (30.4%)	2 (8.7%)	0.19
	No	81 (77.9%)	62 (76.5%)	11 (16.6%)	8 (9.9%)	
Prior hormone therapy	Yes	43 (41.3%)	24 (55.8%)	12 (27.9%)	7 (16.3%)	0.004
	No	61 (58.7%)	52 (85.3%)	6 (9.8%)	3 (4.9%)	
Administered activity		161.1 (27.7)	161.2 (27.0)	167.7 (28.5)	148.7 (29.7)	0.22
Uptake time (mins)		69.6 (10.7)	69.3 (10.7)	67.8 (9)	74.5 (13)	0.27
Indication	Assess recurrence	53 (51%)	41 (77.4%)	7 (13.2%)	5 (9.43%)	
	Primary staging	35 (33.6%)	28 (80%)	6 (17.1%)	1 (2.9%)	
	Others	16	7 (43.8%)	5 (31.2%)	4 (25%)	

Quantitative data presented as Mean (Standard Deviation) while qualitative data presented as Number (%).

*Only one datum available

from the medium, and 1 from the high TB groups. The majority had a Gleason score between 7 and 9 (44/57, 77.2%).

Serum PSA was noted in 102 of 104 patients. PSA was not available in two patients (one from the low and one from the high TB group). There were significantly higher PSA values in the high TB group compared to the low and medium groups. Mean PSA in the high TB group was 214.34 ± 224.09 ng/mL (range 0.76-746.99 ng/mL), whereas the mean PSA for the low and medium TB groups were 16.18 ± 31.13 ng/mL (range 0.003-160.54 ng/mL) and 41.35 ± 49.21 ng/mL (range 0.03-171.21 ng/mL), respectively.

The clinical indications for imaging included assessment for recurrent/metastatic disease (53/104, 51.0%) and primary staging/preoperative evaluation (35/104, 33.7%), among a few others (e.g., PRLT planning and treatment monitoring). All of those referred for assessment of recurrent disease had prior intervention (e.g., surgery, chemotherapy, radiation therapy, and hormone therapy). A statistically significant difference was detected in the proportion of patients who received chemotherapy and prior hormone therapy than those who did not, as seen in Table 1. Other prior interventions showed no significant difference.

PET Imaging

Patients' scans with low administered activities (<100 MBq) or long uptake time (>100 minutes) were excluded for analysis. As a result, no significant differences were observed for AA and UT. Mean AA was 161.1 ± 27.7 MBq (range 100-228 MBq), and mean UT was 69.6 ± 10.7 minutes (range 50-100 minutes).

Tissue uptake

Tracer uptake (SUVmax and SUVmean) in the salivary glands, kidneys, and liver showed a significant reduction in the high tumor burden group compared to the low TB group. Uptake reduction by 25.9% to 27.4% for the parotid glands, 24.8% to 27.3% submandibular glands, 39.4% to 45.8% for the kidneys, and 33.7% to 36.1% for the liver was observed. In general, SUVmean of these organs had more noticeable declines compared to their SUVmax. Kidneys SUVmean exhibited the most prominent drop of 45.8% ($p = 0.002$) between low and high TB groups. Normal tissue uptake results are listed in Table 2; SUVmax and SUVmean are illustrated in Figure 2.

SUVmax in the bone showed a significant increase in patients with high tumor burden compared with low tumor burden. No significant difference was observed for the other normal tissue uptake sites (lacrimal glands, spleen, and bone SUVmean). The lacrimal and salivary glands SUVs could not be delineated in two patients (one from the high TB group and one from the medium TB group) due to low uptake or bone metastases involving the adjacent skull. In five patients belonging to the high TB group, normal bone SUVs could not be measured due to extensive bone metastases.

Correlative Analysis of Tissue Uptake

Weak but significant negative correlations ($rho \approx 0.2$-0.3; $p \leq 0.05$) were noted between TB groups and the SUVmax and SUVmean of the salivary glands, and kidneys. Uptake in the salivary glands, kidneys and liver correlated negatively with serum PSA, a surrogate tumor burden marker ($rho \approx 0.2$-0.3; $p \leq 0.05$). Correlation of SUVmean and PSA is illustrated in Figure 3. PSMA uptake of the kidneys was also noted to have weak but significant positive correlation with weight ($rho \approx 0.2$), not BMI. No significant correlation was noted for the other studied tissues with the other parameters (e.g., AA, UT, weight, and BMI).

DISCUSSION

The rapidly expanding use of PSMA - ligand radiopharmaceuticals in imaging and therapy of patients with prostate cancer is accompanied by the need to understand factors that may affect normal tissue uptake. This retrospective analysis explored the effect of tumor burden on the PSMA uptake in non-target healthy tissues among Filipino patients with prostate cancer. Here, we show the significant impact of high tumor burden on the Ga-68 PSMA I&T uptake of the kidneys, salivary glands, and liver, where mean tracer uptake in these organs was notably reduced approximately 25% to 50% in patients with high tumor burden.

TABLE 2. Normal tissue Ga-68 PSMA uptake across tumor burden groups.

			TUMOR BURDEN			
			Low	Medium	High	P value
	SUV	N	Mean (SD)	Mean (SD)	Mean (SD)	
Lacrimal glands*	max	102	6.77 (3.22)	6.66 (3.34)	5.64 (2.25)	0.605
	mean	102	3.92 (1.86)	3.64 (1.70)	3.28 (1.33)	0.539
Parotid glands*	max	103	16.44 (4.85)	15.50 (4.65)	**12.18 (5.89)**	**0.041**
	mean	103	10.09 (2.94)	9.57 (3.0)	**7.32 (3.71)**	**0.036**
Submandibular glands*	max	103	19.13 (5.24)	16.01 (5.49)	**14.39 (6.54)**	**0.010**
	mean	103	11.66 (3.31)	**9.51 (3.50)**	**8.48 (3.65)**	**0.005**‡
Kidneys†	max	104	47.73 (17.2)	43.20 (14.03)	**28.70 (12.28)**	**0.007**
	mean	104	28.82 (10.71)	26.66 (8.82)	**15.63 (7.58)**	**0.002**§
Liver†	max	104	5.21 (1.65)	5.30 (1.69)	**3.45 (1.80)**	**0.013**
	mean	104	4.06 (1.37)	4.07 (1.34)	**2.59 (1.52)**	**0.011**
Spleen†	max	104	7.60 (2.71)	7.30 (2.92)	8.17 (4.48)	0.835
	mean	104	5.79 (2.08)	5.67 (2.44)	5.97 (3.08)	0.845
Bone†	max	99	1.35 (0.35)	1.43 (0.35)	1.97 (0.66)	0.038
	mean	99	0.81 (0.22)	0.83 (0.22)	1.06 (0.26)	0.059

Legend:

*Normally distributed data: used one-way ANOVA and Tukey-Kramer tests

†Not normally distributed data: used Kruskal-Wallis and Mann-Whitney U tests

Values in bold signify statistically significant reduction of P values (≤ 0.05) between tumor groups and in patients with high and low TB groups

‡Significant difference between medium and low TB groups P values (≤ 0.05)

§Significant difference between medium and high TB groups P values (≤ 0.05)

Similar to the established biodistribution studies of Ga-68 PSMA I&T [5,13] and other PSMA-targeted radiotracers [23-26], the kidneys and the salivary glands exhibited the highest uptake among the studied organs. This is followed by the lacrimal glands, liver, and spleen, and minimal uptake in the bone. Due to the high physiologic uptake of the kidneys and salivary glands, these two have previously been identified as the relevant critical organs or the dose-limiting organs for PRLT [27,28].

Remarkably, these at-risk organs are found to have a significant reduction in uptake with high TB. Despite the patient population being Filipino and predominantly with low TB, our results with ^{68}Ga-PSMA I&T are compatible with previous studies supporting the tumor sink effect using Ga-68 PSMA-11 [19] and Lu-177 PSMA-617 [21,22]. In addition, liver uptake has also shown to be significantly reduced with high TB in the current study. A significant inverse correlation between visual TB and PSA (surrogate tumor burden marker), and uptake in these organs is also noted, although with weak correlation coefficients (rho ≈ 0.2-0.3). A small, positive correlation (rho ≈ 0.2) was also observed between kidney uptake and weight. No significant difference or correlation with tumor burden, PSA, AA, UT, or weight was noted among the other organs studied. These observations remind us that although normal tissue biodistribution may depend on tumor load, several other factors can cause uptake variability. In a study investigating inter-patient and intra-patient variability using a related PSMA-targeted radiotracer 18F-DCFPyl, the intra-patient variability factors mostly influenced liver and kidney uptake,

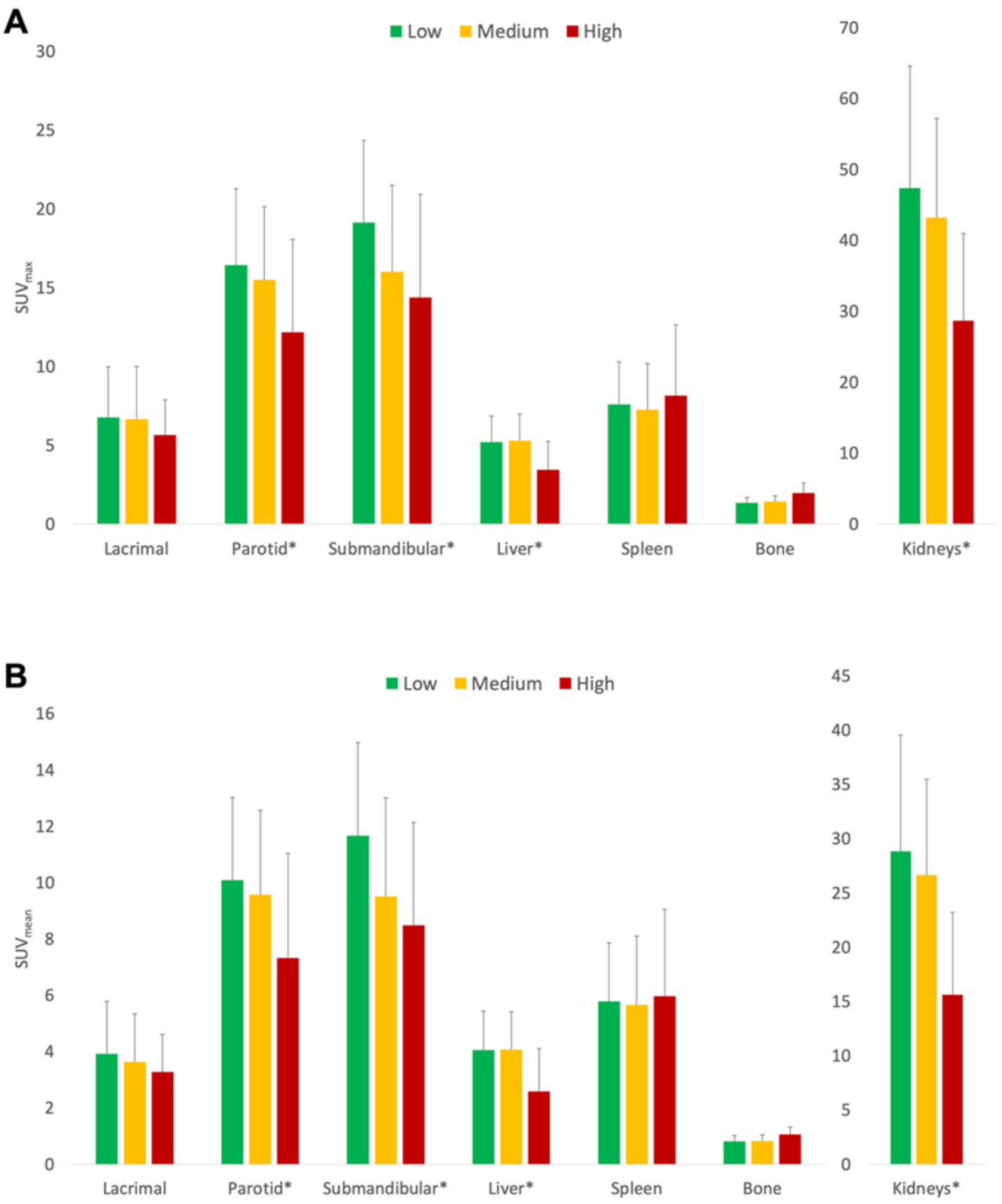

FIGURE 2. Bar graphs showing influence of tumor burden on the 68Ga-PSMA I&T normal tissue uptake (A. SUVmax and B. SUVmean) with error bars (SD), relating to tumor burden groups (low, medium, and high). *Significant reduction ($P \leq 0.05$) of PSMA uptake across TB groups

.

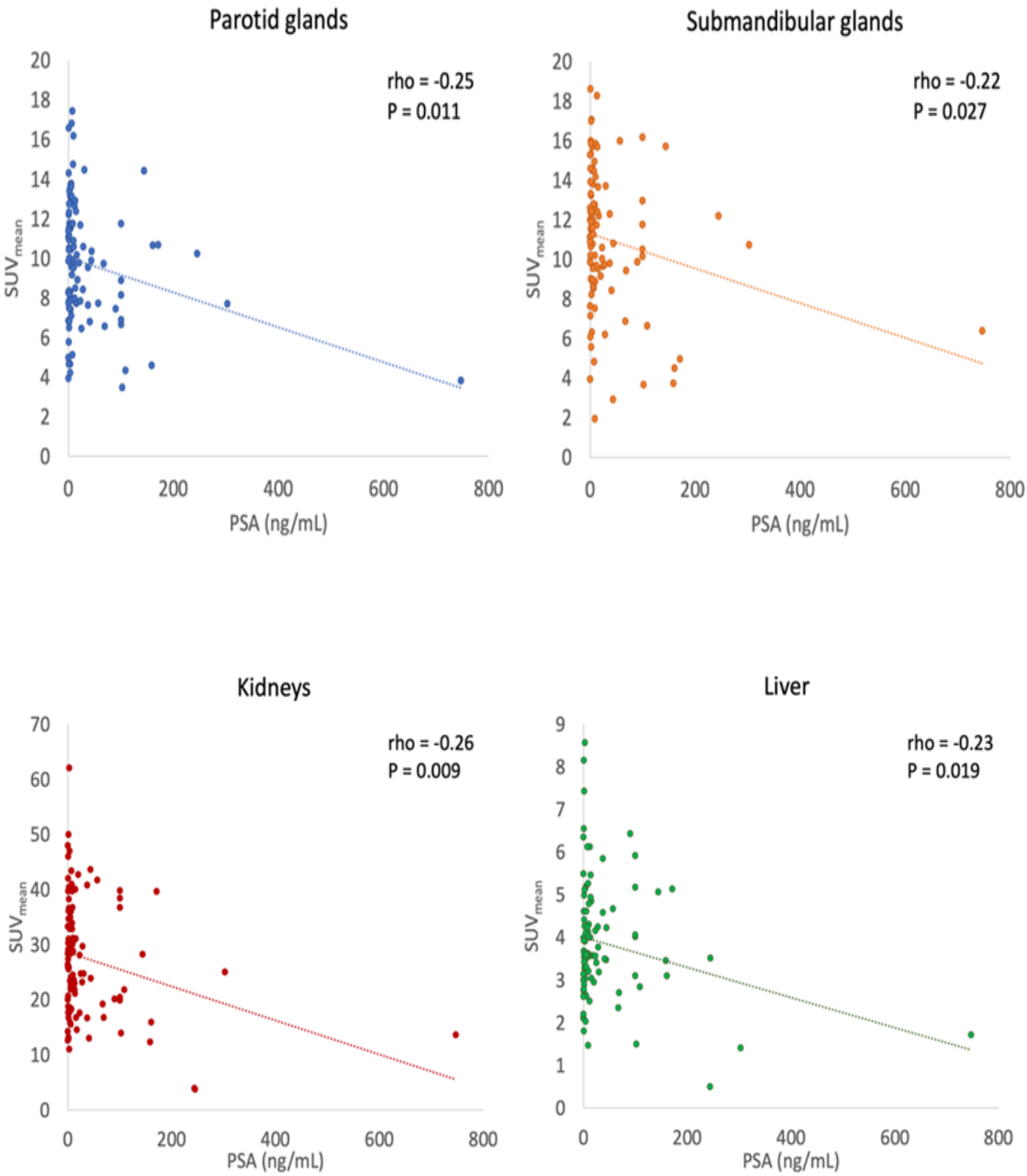

FIGURE 3. Scatter plots showing weak but significant negative correlations of the salivary glands, kidneys, and liver ^{68}Ga-PSMA I&T uptake (SUVmean) with serum PSA. .

and weight. No significant difference or correlation with tumor burden, PSA, AA, UT, or weight was noted among the other organs studied. These observations remind us that although normal tissue biodistribution may depend on tumor load, several other factors can cause uptake variability. In a study investigating inter-patient and intra -patient variability using a related PSMA-targeted radiotracer ^{18}F-DCFPyl, the intra-patient variability factors mostly influenced liver and kidney uptake, whereas inter-patient variability factors largely affected the lacrimal glands, salivary glands, and spleen [29].

While this study focuses mainly on the effect of tumor burden on the biodistribution, there were several attempts to lessen interpatient variability from other factors in the analysis. For example, patients with known or suspected renal impairment and those scanned beyond the institution's standard protocol (low administered activities and prolonged uptake time) were excluded. Moreover, homogeneity of patient characteristics (age, height, weight, BMI, nationality, Gleason score, years since diagnosis, recent PSA value at the time of the scan, and prior interventions) and imaging parameters (AA and UT) were investigated. Baseline characteristics were relatively uniform; only the PSA, prior chemotherapy, and hormone therapy were found to be significantly different, and no significant correlations between tissue uptake and AA nor UT were observed. Conversely, factors that contribute to intra-patient variability (e.g., time of day, recent meals, and hydration status) [29] were not evaluated.

Following the tumor sink effect, all normal tissue uptake should be reduced with high tumor burden. However, this study records a statistically significant increase in patients' normal bone uptake with high tumor burden. This is possibly due to the small number of successfully measured bone uptake in the high TB group, only five out of ten. It may also be potentially caused by the inherent difference of biodistribution in the bone and blood pool of ^{68}Ga-PSMA I&T, which has been shown to have higher retention than ^{68}Ga-PSMA-11 [7]. Additionally, occult skeletal metastases cannot be discounted. Despite being statistically significant, uptake in the bone was found to be minimal in all patients. SUVmean of the bone ranges from 0.19 to 1.74; both the lowest and highest values were found in the low TB group. Further research is suggested to verify this observation and to explore its clinical significance.

This study has several strengths. First, this is the first study evaluating the effect of tumor burden on normal Ga-68 PSMA I&T biodistribution in the Philippines and Filipino patients with prostate cancer. Second, patient homogeneity with baseline characteristics, administered activity, and uptake time for the PET imaging was observed. As a result, the probability of inter-patient variability affecting the outcomes is low. Third, Ga-68 PSMA I&T is the radiopharmaceutical used, reflective of our local real-world scenario, and is likely more representative of its therapeutic arm counterpart's biodistribution. Moreover, all patients were scanned in the same PET/CT scanner assuring uniform SUV measurements.

This study's potential restrictions include visual classification of tumor load instead of quantitative tumor volume measurement as part of our institution's limited workstation capabilities. Also, a large bulk of the patients studied have low tumor load. Nevertheless, this patient population represents our typical patient population, and statistically significant results were observed. Owing to the study's retrospective nature, collected data on the patient's history (e.g., prior intervention and date of initial diagnosis) were vulnerable to recall bias of informants and recorded information by the interviewer. Only single static scans were analyzed, precluding evaluation of intra-patient factors.

Our present analysis shows tumor burden's significant influence on the normal biodistribution of PSMA tracer uptake wherein high tumor burden results in substantially reduced physiologic tissue uptake of the kidneys, salivary glands, and liver. Although extensive research has shown high accuracy, efficacy and safety of ^{68}Ga/^{177}Lu-PSMA theragnostics, limited data are available on factors that may affect the tracers' biodistribution. This is the first study to document such findings in our local setting. As these have implications on possible dose adjustment for PRLT in our local setting, it is highly recommended that subsequent studies investigate tumor load quantitatively and explore other factors that may cause variability of ^{68}Ga/^{177}Lu-PSMA biodistribution.

CONCLUSION

Significantly reduced 68Ga-PSMA I&T uptake is observed in the kidneys, the salivary glands and the liver in patients with high tumor burden. As ^{68}Ga and ^{177}Lu-PSMA I&T have comparable biodistribution, this study has significant implications on PSMA-targeted radionuclide therapy. It corroborates the hypothesis that

patients with higher tumor load can tolerate higher activity doses of 177Lu-PSMA for radionuclide therapy before developing significant damage to the critical organs. Further studies are needed to extrapolate these data in optimizing and personalizing ^{177}Lu-PSMA I&T dose for PRLT.

ACKNOWLEDGMENT

The authors would like to thank Jordan P. Santos, data scientist and biostatistician, for providing statistical analysis.

REFERENCES

1. The Global Cancer Observatory, 608-Philippines-Fact-Sheets. [pdf] International Agency for Research on Cancer. World Health Organization. 2018. Available from: <https://gco.iarc.fr/today/data/ factsheets/populations/608-philippines-fact-sheets.pdf>.
2. Wright GL Jr, Haley C, Beckett ML, Schellhammer PF. Expression of prostate-specific membrane antigen in normal, benign, and malignant prostate tissues. Urol Oncol. 1995;1 (1):18-28. doi:10.1016/1078-1439(95)00002-y.
3. Santoni M, Scarpelli M, Mazzucchelli R, et al. Targeting prostate-specific membrane antigen for personalized therapies in prostate cancer: morphologic and molecular backgrounds and future promises. J Biol Regul Homeost Agents. 2014;28(4):555-563.
4. Jones W, Griffiths K, Barata PC, Paller CJ. PSMA Theranostics: Review of the Current Status of PSMA-Targeted Imaging and Radioligand Therapy. Cancers (Basel). 2020;12(6):1367. Published 2020 May 26. doi:10.3390/cancers12061367.
5. Weineisen M, Schottelius M, Simecek J, et al. ^{68}Ga- and ^{177}Lu-Labeled PSMA I&T: Optimization of a PSMA-Targeted Theranostic Concept and First Proof-of-Concept Human Studies. J Nucl Med. 2015;56(8):1169-1176. doi:10.2967/jnumed.115.158550.
6. Virgolini I, Decristoforo C, Haug A, et al. Current status of theranostics in prostate cancer. Eur J Nucl Med Mol Imaging 2018;45, 471–495. https://doi.org/10.1007/s00259-017-3882-2.
7. McCarthy M, Langton T, Kumar D, Campbell A. Comparison of PSMA-HBED and PSMA-I&T as diagnostic agents in prostate carcinoma. Eur J Nucl Med Mol Imaging. 2017;44(9):1455-1462. doi:10.1007/s00259-017-3699-z.
8. Berliner C, Tienken M, Frenzel T, et al. Detection rate of PET/CT in patients with biochemical relapse of prostate cancer using [^{68}Ga]PSMA I&T and comparison with published data of [^{68}Ga]PSMA HBED-CC. Eur J Nucl Med Mol Imaging. 2017;44(4):670-677. doi:10.1007/s00259-016-3572-5.
9. Ukihide Tateishi, Prostate-specific membrane antigen (PSMA)–ligand positron emission tomography and radioligand therapy (RLT) of prostate cancer, Japanese Journal of Clinical Oncology, Volume 50, Issue 4, April 2020, Pages 349–356, https://doi.org/10.1093/jjco/hyaa004.
10. Emmett L, Willowson K, Violet J, Shin J, Blanksby A, Lee J. Lutetium ^{177} PSMA radionuclide therapy for men with prostate cancer: a review of the current literature and discussion of practical aspects of therapy. J Med Radiat Sci. 2017;64(1):52-60. doi:10.1002/jmrs.227
11. van Kalmthout LWM, van der Sar ECA, Braat AJAT, et al. Lutetium-177-PSMA therapy for prostate cancer patients—a brief overview of the literature. Tijdschr Urol 2020;10, 141–146. https://doi.org/10.1007/s13629-020-00300-z.
12. Afshar-Oromieh A, Malcher A, Eder M, et al. PET imaging with a [^{68}Ga]gallium-labelled PSMA ligand for the diagnosis of prostate cancer: biodistribution in humans and first evaluation of tumour lesions [published correction appears in Eur J Nucl Med Mol Imaging. 2013 May;40(5):797-8]. Eur J Nucl Med Mol Imaging. 2013;40 (4):486-495. doi:10.1007/s00259-012-2298-2.
13. Herrmann K, Bluemel C, Weineisen M, et al. Biodistribution and radiation dosimetry for a probe targeting prostate-specific membrane antigen for imaging and therapy. J Nucl Med. 2015;56(6):855-861. doi:10.2967/jnumed.115.156133
14. Bautista PA. The Emergence of Theranostics in the Philippines: Overcoming Challenges and Bringing Hope. Nucl Med Mol Imaging. 2019;53(1):30-32. doi:10.1007/s13139-018-0560-7.
15. Emmett L, Willowson K, Violet J, Shin J, Blanksby A, Lee J. Lutetium-177 PSMA radionuclide therapy for men with prostate cancer: a review of the current literature and discussion of practical aspects of therapy. J Med Radiat Sci. 2017;64(1):52-60. doi:10.1002/jmrs.227
16. Zuckier L, Martineau P. Altered Biodistribution of Radiopharmaceuticals Used in Bone Scintigraphy. Seminars in nuclear medicine. 2015;45. 81-96. doi:10.1053/j.semnuclmed.2014.07.007.
17. Manov JJ, Roth PJ, Kuker R. Clinical Pearls: Etiologies of Superscan Appearance on Fluorine-18-Fludeoxyglucose Positron Emission Tomography - Computed Tomography. Indian J Nucl Med. 2017;32(4):259-265. doi:10.4103/ijnm.IJNM_56_17
18. Beauregard JM, Hofman MS, Kong G, Hicks RJ. The tumour sink effect on the biodistribution of ^{68}Ga-DOTA-octreotate: implications for peptide receptor radionuclide therapy. Eur J Nucl Med Mol Imaging. 2012;39(1):50-56. doi:10.1007/s00259-011-1937-3

19. Gaertner FC, Halabi K, Ahmadzadehfar H, et al. Uptake of PSMA-ligands in normal tissues is dependent on tumor load in patients with prostate cancer. Oncotarget. 2017;8 (33):55094-55103. Published 2017 Jul 6. doi:10.18632/ oncotarget.19049.
20. Werner RA, Bundschuh RA, Bundschuh L, et al Semiquantitative Parameters in PSMA-Targeted PET Imaging with [^{18}F]DCFPyL: Impact of Tumor Burden on Normal Organ Uptake. Mol Imaging Biol. 2020;22(1):190-197. doi:10.1007/s11307-019-01375-w.
21. Filss C, Heinzel A, Miiller B, Vogg ATJ, Langen KJ, Mottaghy FM. Relevant tumor sink effect in prostate cancer patients receiving ^{177}Lu-PSMA-617 radioligand therapy. RelevanteSenkung der TumorlastbeiProstatakarzinom-Patientenunter der Gabe von ^{177}Lu-PSMA-617. Nuklearmedizin. 2018;57(1):19-25. doi:10.3413/ Nukmed-0937-17-10.
22. Violet J, Jackson P, Ferdinandus J, et al. Dosimetry of ^{177}Lu-PSMA-617 in Metastatic Castration-Resistant Prostate Cancer: Correlations Between Pretherapeutic Imaging and Whole-Body Tumor Dosimetry with Treatment Outcomes. J Nucl Med. 2019;60(4):517-523. doi:10.2967/jnumed.118.219352.
23. Kurash MM, Gill R, Khairulin M, et al. ^{68}Ga-labeled PSMA-11 (68Ga-isoPROtrace-11) synthesized with ready to use kit: normal biodistribution and uptake characteristics of tumour lesions. Sci Rep 2020;10, 3109. https:// doi.org/10.1038/s41598-020-60099-y.
24. Ferreira G, Iravani A, Hofman MS, et al. Intra-individual comparison of ^{68}Ga-PSMA-11 and ^{18}F-DCFPyL normal - organ biodistribution. Cancer Imaging 2019;19, 23. doi: 10.1186/s40644-019-0211-y
25. McCarthy M, Langton T, Kumar D, Campbell A. Comparison of PSMA-HBED and PSMA-I&T as diagnostic agents in prostate carcinoma. European Journal of Nuclear Medicine and Molecular Imaging. 2017 Aug;44(9):1455-1462. doi: 10.1007/s00259-017-3699-z.
26. Li X, Rowe SP, Leal JP, et al. Semiquantitative Parameters in PSMA-Targeted PET Imaging with ^{18}F-DCFPyL: Variability in Normal-Organ Uptake. J Nucl Med. 2017;58(6):942-946. doi:10.2967/jnumed.116.179739.
27. Kabasakal L, AbuQbeitah M, Aygün A, et al. Pre-therapeutic dosimetry of normal organs and tissues of (177)Lu-PSMA-617 prostate-specific membrane antigen (PSMA) inhibitor in patients with castration-resistant prostate cancer. Eur J Nucl Med Mol Imaging. 2015;42 (13):1976-1983. doi:10.1007/s00259-015-3125-3.
28. Okamoto S, Thieme A, Allmann J, et al. Radiation Dosimetry for ^{177}Lu-PSMA I&T in Metastatic Castration - Resistant Prostate Cancer: Absorbed Dose in Normal Organs and Tumor Lesions. J Nucl Med. 2017;58(3):445-450. doi:10.2967/jnumed.116.178483.
29. Sahakyan K, Li X, Lodge MA, et al. Semiquantitative Parameters in PSMA-Targeted PET Imaging with [^{18}F] DCFPyL: Intrapatient and Interpatient Variability of Normal Organ Uptake. Mol Imaging Biol. 2020;22(1):181-189. doi:10.1007/s11307-019-01376-9.

transmedic
advancing medical technologies

NUCLEAR MEDICINE PRODUCT PORTFOLIO

SPECTRUM DYNAMICS MEDICAL

Future-proof Cadmium Zinc Telluride (CZT) based cardiac and nuclear medicine imaging system

D-SPECT CARDIO®

UNITED IMAGING

Ultra-High-Resolution Digital PET/CT with 194 cm Axial FOV

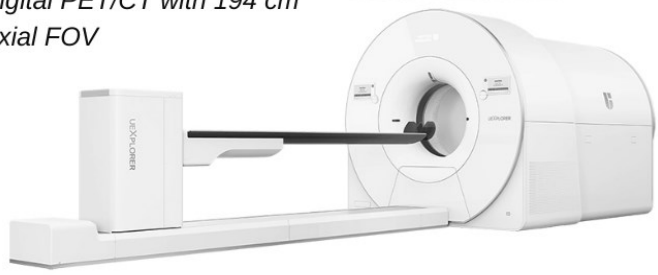

DDD Diagnostic

Gamma Camera for General Purpose Nuclear Medicine

CMR NAVISCAN

Breast-Dedicated Radionuclide Imaging system

Australian Government | ANSTO

Science. Ingenuity. Sustainability.

Sterile Tc-99m Generator

Eckert & Ziegler

Contributing to saving lives

Your one-stop-shop for the complete synthesis: from radionuclides to radiosynthesis and its quality control

BEST ABT MOLECULAR IMAGING

Dose on Demand Biomarker Generator

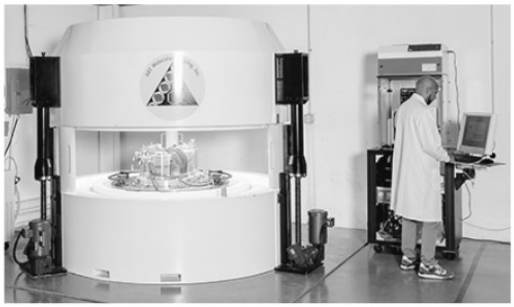

mim Encore

A Comprehensive Solution for PET and Nuclear Medicine

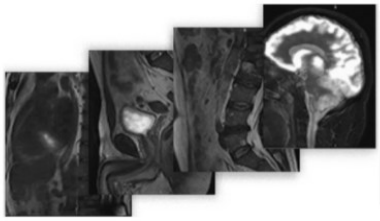

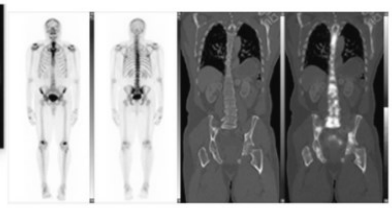

Bone mineral density change after chemotherapy in Filipino premenopausal patients treated for early breast cancer at JRRMMC

Venus S. Fortuna, MD, Marcelino A. Tanquilut, MD, Emelito O. Valdez-Tan, MD,
Wenceslao S. Llauderes, MD

Department of Nuclear Medicine , Jose R Reyes Memorial Medical Center
E-mail address: venusnucmed@gmail.com, m_tanquilut@gmail.com, valdeztan@yahoo.com , doc_wesley@yahoo.com

ABSTRACT

Background:

According to GLOBOCAN 2008, Breast cancer was the leading cause of morbidity (12,262) and mortality (4,371) among Filipino women in the Philippines. Ten years later, it is still on the top of the chart in terms of incidence (24,798), mortality (8,057) and five-year prevalence (68,537). Over the years, survival from breast cancer has improved with earlier diagnosis and advanced medical treatments, thus it is becoming important to monitor for potentially detrimental effects, such as osteoporosis. The reference standard method evaluating osteoporosis is by measuring bone mineral density (BMD) by Dual Energy X-ray Absorptiometry (DXA) scanner. Studies on the impact of chemotherapy in the BMD of premenopausal breast cancer patients have been studied among Europeans, Americans, Mexicans, and others, but there is a lack of information in the Filipino population.

Objective:

The study aimed to determine the bone mineral density (BMD) change after chemotherapy in Filipino premenopausal patients treated for early breast cancer.

Methods:

A longitudinal, prospective study design was applied with measurements before and after chemotherapy treatment in 28 premenopausal patients with early breast cancer. This study done with the approval of the ethical board of the Institutional Review Board of Jose R. Reyes Memorial Medical Center from January 2019 to January 2020. BMD measurements were taken by Dual Energy X-ray Absorptiometry (DXA) scans before and after completion of chemotherapy (6 months). Patients' clinical data was recorded. Fischer exact test was utilized to analyze the association of age and menstruation status. Independent t-test was used to compare the mean BMD and menstruation status. Paired T-Test was used to compare BMD before and after chemotherapy The level of statistical significance was set at $p \leq 0.05$, while Medcalc Statistical software version 19.3.1 was used to carry out statistical calculations. The major limitation of this study was the time constraints in getting more participants who are willing to join and will be less likely to be excluded in the future. Catastrophic natural events like volcanic eruption and COVID-19 pandemic also became a major hindrance to gathering participants.

Results:

28 eligible patients volunteered for the study. The final analysis included 11 patients with mean age of 40.4 ± 6.5 with breast cancer (stage IIA-IIIB) who had 2 DXA scans. The results showed significant decrease in the Z-score of the lumbar spine by 64.3% after chemotherapy ($p=0.0328$). We observed no significant decrease in the Z-score of the femoral neck. The age of the patients, whether below 40 or above 40 years old, as well as the bone mineral density in the lumbar spine and femoral neck, were not associated with the menstruation status, whether the patients developed transient or continuous amenorrhea during and after chemotherapy. There was no significant change in the body mass index before and after chemotherapy, ($p=0.4284$).

Conclusions:

This study showed significant decrease in the Z-score of the lumbar spine after chemotherapy. The BMD in the lumbar spine and femoral neck decreased after chemotherapy, however the change was not significant. The age and the mean BMD of the patients were not associated with the menstruation status during and after chemotherapy. DXA may benefit breast cancer patients who will undergo chemotherapy about their bone health.

Keywords*: Bone Mineral Density, DXA, Premenopausal, Breast Cancer , Filipino*

INTRODUCTION

According to GLOBOCAN 2008, Breast cancer was the leading cause of morbidity (12,262) and mortality (4,371) among Filipino women in the Philippines. Ten years later, it is still on the top of the chart in terms of incidence (24,798), mortality (8,057) and five-year prevalence (68,537) [1,2]. Over the years, survival from breast cancer has improved with earlier diagnosis and advanced medical treatments, thus it is becoming important to monitor for potentially detrimental effects, such as osteoporosis. The reference standard method evaluating osteoporosis is by measuring bone mineral density (BMD) by Dual Energy X-ray Absorptiometry (DXA) scanner, which measures the bone in grams per square centimeter.

At present, premenopausal patients with early stage breast cancer are treated with chemotherapy with a combination of drugs such as cyclophosphamide, doxorubicin, and docetaxel that can cause ovarian failure and premature menopause, resulting to chemotherapy induced bone loss [3]. In literature, there are variable results about the effects of chemotherapy in the bone mineral density of premenopausal women and there is no standard timing for taking the post chemotherapy DXA scan [4 - 12] .

Studies on the impact of chemotherapy in the BMD of premenopausal breast cancer patients have been studied among Europeans, Americans, Mexicans, and others, but there is a lack of information in the Filipino population.

MATERIALS AND METHODS

The research design was based on a longitudinal, prospective study of premenopausal women below 50 years old with primary diagnosis of early invasive breast cancer who are being treated at Jose R. Reyes Memorial Medical Center (JRRMMC), a tertiary level medical center in Manila, Philippines. With the approval of the ethical board of the Institutional Review Board of JRRMMC, patients' data were gathered with permission from the files of the Medical Oncology Department. This study was conducted between January 2019 to January 2020. The women included in this study were aged below fifty (50) years old, premenopausal, and diagnosed with early breast cancer (stage 0, IA-IB), stage II (A-B) and III (A-B), without comorbidities that may affect body or bone composition such as endocrine disorders, skeletal deformities, second primary cancer, and no previous chemotherapy, who responded to invitations via text messaging and phone call. Excluded in the analysis were women who showed bone metastases on bone scan, discontinued their chemotherapy, had salphingoophorectomy, or were lost to follow up.

The women who responded to the invitation were requested to sign an informed consent for study participation and Dual Energy X-Ray Absorptiometry (DXA) scan. Information about their demographic data, clinical staging, medical history, height and weight, menstrual history (menstruation cycle before treatment, during and after treatment), history of smoking and alcoholic beverage drinking, and comorbidities, and intake of any medications were recorded on their DXA interview sheet.

Bone Mineral Density (BMD) was measured using the same Dual Energy X-Ray Absorptiometry (Hologic Discovery Wi) scanner at the Nuclear Medicine department of JRRMMC. The DXA scan protocol was in accordance to the guidelines set by the International Society for Clinical Densitometry (ISCD) and was performed by a trained and certified technical staff. The quality standards of the scanner was tested daily. BMD measurements from the lumbar spine (L1-L4) and femoral neck were taken before chemotherapy and after completion of chemotherapy. The results of the BMD were reported in grams per square centimeter (g/cm2). For premenopausal women, the Z-score was used to calculate the BMD using the WHO criteria where, Z-score of negative 2.0 or less is "below the expected range for age" and Z-score above -2.0 is "within the expected range for age". The Z-score describes the standard deviations by which the BMD of an individual is compared to the mean value expected for age and

gender. The DXA scan results were interpreted by at least two board certifies nuclear medicine physicians as a consensus in accordance with the guidelines specified by the ISCD.

Statistical Analysis

Descriptive statistics such as mean and standard deviation were used to present continuous variables such as age, BMI and BMD. The rest of the categorical data were presented by frequency and percentage. Fischer exact test was utilized in determining the association of age and menstruation status while independent t - test was used to compare the mean BMD between patients who reported transient amenorrhea and continuous after chemotherapy. BMD before and after chemotherapy were compared using paired T - Test. The level of statistical significance was set at $p \leq 0.05$, while Medcalc Statistical software version 19.3.1 was used to carry out statistical calculations.

RESULTS

With informed consent, a total of 28 eligible volunteers with age ranging from 29 to 49 years old (mean age 40.4 ± 6.5) diagnosed with early breast cancer, underwent DXA scan prior to chemotherapy. Only 11 patients completed both the baseline and the second DXA after completing the chemotherapy. The drop outs were mostly due to lost to follow up (9), three (3) presented with bone metastases on bone scan and four (4) died. The characteristics and clinicopathologic features of the patients in the final analyses are presented in Table 1. The baseline BMI of the patients were mostly normal (7 (63.6%), 3 (27.3%) were overweight, and 1 (9.1%) was obese. Three out of 11 already had surgical removal of the breast. All tumors (100%) were invasive ductal carcinomas, with 4 (36.4%) stage IIA, 2 (18.2%) stage IIB, 3 (27.3%), 3 (27.3) stage IIIA, and 2 (18.2) stage IIIB. None of our patients were smokers and alcoholic beverage drinkers nor had any comorbidities. Ten (10) patients completed 4 cycles of chemotherapy combination of Doxorubicin - Cyclophosphamide and another 4 cycles of Docetaxel, while 1 patient underwent 4 cycles of Doxorubicin-Cyclophosphamide and 4 cycles of Taxane – Trastuzumab. On their baseline DXA scan, 10 out of 11 patients had a Z-score that was "within the expected range for age" in the lumbar spine and femoral neck. Only one patient had Z-score that was "below the expected range for age" in the same skeletal sites.

In Table 2, age, BMD, and mestrual status were shown. Two out of 11 (18.18%) patients have stopped menstruating during and after chemotherapy. The rest of the patients (9/11) developed transient amenorrhea during their treatment. Results showed that age below or above 40 years old was not associated with the menstrual status ($p = 1.000$). In the same table, result showed that the mean BMD in the lumbar spine ($p = 0.5707$) and femoral neck ($p = 0.5241$) had no significant association menstruation status whether the patient developed transient amenorrhea during chemotherapy or continued to experience amenorrhea after chemotherapy.

Comparing the BMD before and after chemotherapy in Table 3 revealed a 1.4% change in the mean BMD in the femoral neck, but the result was not significant ($p = 0.2368$). In the lumbar spine, the 5.2% decrease was also not significant ($p = 0.066$). Comparing The mean Z-score before and after chemotherapy, there was a 10.1% decrease in the femoral neck, but the change was not significant ($p = 0.1500$). On the other hand, the mean Z-score in the lumbar spine showed a significant decrease of 64.3% ($p = 0.0328$). Finally, the results also showed no significant change in the body mass index before after chemotherapy ($p = 0.4284$).

DISCUSSION

Chemotherapeutic agents such as doxorubicin, cyclophosphamide, and docetaxel are known to induce ovarian failure and amenorrhea, leading to bone loss often referred to with chemotherapy induced bone loss in premenopausal patients treated with these agents [3 - 7, 9 - 15]. The rapid decline in estrogen levels increases the level of bone turnover is seen as decrease in bone mineral density in DXA scan [5].

TABLE 1. Patient characteristics and clinicopathologic features

	Respondents (n=11)	**Drop Outs** (n=17)
Age (Mean)	40.4 ± 6.5	42.0 ± 5.0
Range (29-49)		
Baseline Body Mass Index (kg/m^2, mean)	24.4 ± 3.3	26.9 ± 4.4
Normal	7 (63.6)	7 (41.2)
Obese	1 (9.1)	4 (23.5)
Overweight	3 (27.3)	6 (35.3)
Clinical Breast Cancer stage		
I	0 (0.0)	1 (5.9)
IIA	4 (36.4)	6 (35.3)
IIB	2 (18.2)	2 (11.8)
IIIA	3 (27.3)	3 (17.6)
IIIB	2 (18.2)	5 (29.4)
Histologic subtype		
Invasive Ductal Carcinoma (IDCA)	11 (100.0)	17 (100.0)
Surgical Status		
Modified Radical Mastectomy	3 (27.3)	7 (41.2)
No surgery	8 (72.7)	10 (58.8)
Lifestyle & Comorbidities		
Smoker	0 (0.0)	0 (0.0)
Alcoholic Beverage drinker	0 (0.0)	0 (0.0)
Comorbidities	0 (0.0)	0 (0.0)
Chemotherapy Regimen		
4 cycles Doxorubicin -Cyclophosphamide	1 (9.1)	-
4 cycles Taxane – Trastuzumab	1 (9.1)	-
4 cycles Doxorubicin - Cyclophosphamide	10 (90.9)	-
4 cycles Docetaxel	10 (90.9)	-
Baseline Bone Mineral Density (BMD) Z-score		
(Lumbar Spine)		
Above -2.0 “Within the expected range for age”	10 (90.9)	14 (87.5)
-2.0 or lower “Below the expected range for age”	1 (9.1)	2 (12.5)
(Femoral Neck)		
Above -2.0 “Within the expected range for age”	10 (90.9)	15 (93.8)
-2.0 or lower “Below the expected range for age”	1 (9.1)	1 (6.3)

Our data showed a 5.2 percent decrease in mean BMD in the lumbar spine after chemotherapy. This result was not statististically significant but is comparable to other studies who evaluated the BMD in the same skeletal site and the same interval of DXA scan of 6 months post chemotherapy. Studies conducted by Shapiro et al. and Cameron et al reported lumbar spine BMD loss of 4% [6,16] while Monroy et al. reported a decrease of almost 5% in the same site [10].

Our results also showed a significant decrease of 64.3% in the Z-score of the lumbar spine which reflects the patients' BMD compared to normal women of the same age, race, and gender in which the score was calculated from the observed value, mean of sample, and standard deviation of the sample. A low Z-score also indicates low bone density. Contrary to the results of other studies [6, 10, 16], we did not observe a significant decrease in the mean BMD and Z-score in the femoral neck. However, even if we look at the Z-score of individual skeletal site, the reporting of the BMD according to ISCD guidelines [17] takes into account at least 2 skeletal sites. We also report that the changes in the BMD and Z-scores in this study is not associated with the age of the patients and whether the they experienced transient amenorrhea during chemotherapy or continued to have amenorrhea after chemotherapy.

We looked into BMI as a factor that may influence the bone mineral density. According to studies, BMD was found to be higher in obese premenopausal women than normal weight and postmenopausal women [14] and was considered a determining factor for BMD in another study among healthy Indian premenopausal women [8]. However, it was also noted that it could be variable in different ethnic groups. Majority or 7 out of 11 of the premenopausal women in our study had normal weight before their chemotherapy and did not show any significant decrease in their BMI after their treatment.

Smoking and alcoholic beverage drinking are known independent risk factors for low bone mineral density depending on the frequency and amount of intake [18], while taking calcium supplements is said to increase BMD and have a significant protective effect on the femur, but not the lumbar spine, according to Monroy et al [10]. None of our patients said they were smokers or alcohol beverage drinkers nor taking calcium supplements before or during their chemotherapy. Some cancer centers give, prednisolone together with chemotherapy with a typical dose of 175 mg for once cycle and receive as much as 1425 mg of the drug over an 18-week treatment period. Fracture risk increases with dose and length of time of intake, especially within the first 3 to 6 months [5]. Patients in our study did not report intake of glucocorticoids during their treatments.

The decrease in BMD and Z-score post chemotherapy could be explained by the normal composition of the skeletal sites we measured and the rate of turnover in these sites. The lumbar spine is 85% trabecular tissue while the femoral neck is 30-50% trabecular tissue. 25 percent of this type of tissue undergoes resorption annually, with estrogen being a key factor in maintaining the balance of resorption and remodeling in the bone [10]. Chemotherapeutic agents that induce ovarian failure are contributory to bone resorption.

One might conclude that BMD loss is irrelevant in Filipino premenopausal women undergoing chemotherapy for breast cancer and that DXA scan is not so important to request early on due to its additional cost and limited availability. But then, a baseline DXA scan may detect low bone mineral density early during their treatment and these patients may benefit from proper diagnosis which otherwise may have an impact in their long-term quality of life. The advantage of this study is the patients' compliance to follow-up DXA since the cost of the scan was covered by a government health program.

We did not explore the diet and physical activity of the patients, which are known to influence bone health. Finally, The major limitation of this study was the small sample size that was due to time constraints in getting more patients to join the study. The unexpected turn of

of the events during the year such as major volcanic eruption in the nearby city and COVID-19 pandemic was the greatest hindrance to gathering participants.

CONCLUSIONS

In this study among 11 premenopausal women with ealy breast cancer, where DXA scan was taken before and after chemotherapy, the results showed that the decrease in the BMD after chemotherapy in the femoral neck and lumbar spine were not statistically significant. The individual Z-scores of the 2 skeletal sites showed significant decrease in the lumbar spine after chemotherapy. Reporting of BMD follows ISCD guidelines using 2 skeletal sites instead of one.

The age and the mean BMD of the patients were not associated with the menstruation status during and after chemotherapy. Our data suggests that a DXA scan may not be necessary before the chemotherapy of premenopausal Filipino women with early breast cancer but recommending it to reassure patients about their bone health will be beneficial. With limited sample size, it is recommended that a similar study be conducted with greater number of participants.

TABLE 2. Association Association between the age and BMD to menstruation status during and after chemotherapy (n=11)

	Transient amenorrhea during chemotherapy n(%)	**Amenorrhea during and after chemotherapy n(%)**	**p value ≤ 0.05**
Age			
Above 40	4 (44.4)	1 (50.0)	
40 and below	5 (55.6)	1 (50.0)	1.0000^{ns}
BMD Lumbar Spine L1-L4	0.91 ± 0.09	0.96 ± 0.16	0.5707 ^{ns}
BMD Femoral neck	0.73 ± 0.07	0.69 ± 0.06	0.5241^{ns}

TABLE 3. Association BMD and BMI measurements before and after chemotherapy (n=11)

	Before Chemo		**After Chemo**				
	Mean ± SD	**Range**	**Mean ± SD**	**Range**	**Difference**	**% change**	**p value**
BMD g/cm^2							
Femoral neck	0.73 ± 0.06	0.58 to 0.83	0.72 ± 0.07	0.60 to 0.81	-0.01	-1.4%	0.2368 ^{ns}
Lumbar spine	0.97 ± 0.11	0.81 to 1.17	0.92 ± 0.09	0.77 to 1.07	-0.05	-5.2%	0.0668^{ns}
Z-score							
Femoral neck	-0.79 ± 0.61	-2.0 to 0.0	-0.87 ± 0.55	-2.0 to -0.3	-0.08	-10.1%	0.1500^{ns}
Lumbar Spine	-0.42 ± 1.05	-2.0 to 1.2	-0.69 ± 0.92	-2.0 to 0.9	-0.27	-64.3%	0.0328*
BMI kg/m^2	24.4 ± 3.3	19.5 to 30	24.27 ± 2.4	21.5 to 28.9	- 0.13	-0.53%	0.4284^{ns}

ACKNOWLEDGEMENT

Special thanks to all the patients who participated in this study, and to the doctors, nurses, and secretaries of the Department of Oncology, Jose Reyes Memorial Medical Center, for each of their contribution to make this project possible.

Special thanks to the Nuclear Med technologists particularly Christopher Eduarte, Angielyn Abad, Novy Jean dela Cruz, June Ann Berdan, and Aja Corine Abela, and co-residents of the Jose R. Reyes Memorial Medical Center, Department of Nuclear Medicine for their great support in this study.

REFERENCES

1. Maghraoui, A.E., Roux,C. DXA scanning in clinical practice, QJM: An International Journal of Medicine, Volume 101, Issue 8, 1 August 2008, Pages 605–617, https://doi.org/10.1093/qjmed/hcn022 .
2. Mazocco, L., & Chagas, P. (2017). Association between body mass index and osteoporosis in women from northwestern Rio Grande do Sul. Revista Brasileira De Reumatologia (English Edition), 57(4), 299-305. doi:10.1016/j.rbre.2016.10.002.
3. Choksi, P., Williams, M., Clark, P. M., & Van Poznak, C. (2013). Skeletal Manifestations of Treatment of Breast Cancer. Current Osteoporosis Reports, 11(4), 319–328. http://doi.org/10.1007/s11914-013-0179-7
4. Bruning, P. F., Pit, M. J., de Jong-Bakker, M., van den Ende, A., Hart, A., & van Enk, A. (1990). Bone mineral density after adjuvant chemotherapy for premenopausal breast cancer. British Journal of Cancer, 61(2), 308–310.
5. Christensen, C. O., Cronin-Fenton, D., Froslev, T., Hermann, A. P., & Ewertz, M. (2016). Change in bone mineral density during adjuvant chemotherapy for early-stage breast cancer. Supportive Care in Cancer, 24, 4229–4236. http://doi.org/10.1007/s00520-016-3250-y.
6. Cameron, D. A., Douglas, S., Brown, J. E., & Anderson, R. A. (2010). Bone mineral density loss during adjuvant chemotherapy in pre-menopausal women with early breast cancer: Is it dependent on oestrogen deficiency? Breast Cancer Research and Treatment, 123 (3), 805-814. doi:10.1007/s10549-010-0899-7.
7. Fogelman I., Blake G.M., Blamey R., Palmer, M., Sauerbrei, W., Schumacher, M., Serin, D., Stewart, A., Wilpshaar, W. Bone mineral density in premenopausal women treated for node-positive early breast cancer with 2 years of goserelin or 6 months of cyclophosphamide, methotrexate and 5-fluorouracil (CMF). Osteoporos Int. 2003 Dec;14(12):1001-6. Epub 2003 Oct 3. PubMed PMID: 14530912.
8. Kumar, A., Sharma, A. K., Mittal, S., & Kumar, G. (2016). The Relationship Between Body Mass Index and Bone Mineral Density in Premenopausal and Postmenopausal North Indian Women. Journal of obstetrics and gynaecology of India, 66(1), 52–56. https://doi.org/10.1007/s13224-014-0629-x.
9. Mc Cune J.S., Games D.M., Espirito, J.L. Assessment of ovarian failure and osteoporosis in premenopausal breast cancer survivors. J Oncol Pharm Pract. 2005 Jun;11(2):37-43. PubMed PMID: 16460603.
10. Monroy-Cisneros, K., Esparza-Romero, J., Valencia, M. E., Guevara-Torres, A. G., Méndez-Estrada, R. O., Anduro-Corona, I., & Astiazarán-García, H. (2016). Antineoplastic treatment effect on bone mineral density in Mexican breast cancer patients. BMC Cancer, 16, 860. http://doi.org/10.1186/s12885-016-2905-x.
11. Partridge, A. H. (2015). Chemotherapy in Premenopausal Breast Cancer Patients. Breast Care, 10(5), 307–310. http://doi.org/10.1159/000441371
12. Ramin, C., May, B.J., Roden, R.B.S., Orellana, M.M., et al. (2018) Evaluation of osteopenia and osteoporosis in younger breast cancer survivors compared with cancer-free women: a prospective cohort study. Breast cancer Research, 20(1). https://doi.org/10.1186/s13058-018-1061-4.
13. Fawzy, T., Muttappallymyalil, J., Sreedharan, J., Ahmed, A., Alshamsi, S. O., Mariyam Saif Salim Humaid Bin Bader Al Ali, & Balsooshi, K. A. (2011). Association between Body Mass Index and Bone Mineral Density in Patients Referred for Dual-Energy X-Ray Absorptiometry Scan in Ajman, UAE. Journal of Osteoporosis, 2011, 1-4. doi:10.4061/2011/876309
14. Salamat MR, Salamat AH, Janghorbani M. Association between Obesity and Bone Mineral Density by Gender and Menopausal Status. Endocrinol Metab (Seoul). 2016 Dec;31(4):547-558. doi:10.3803/EnM.2016.31.4.547. Epub 2016 Nov 4. PMID: 27834082; PMCID: PMC5195832.
15. Swain, S. M., Land, S. R., Ritter, M. W., Costantino, J. P., Cecchini, R. S., Mamounas, E. P., Wolmark, N., & Ganz, P. A. (2009). Amenorrhea in premenopausal women on the doxorubicin and cyclophosphamide followed by docetaxel arm of NSABP B-30 trial. Breast cancer research and treatment, 113(2), 315–320. https://doi.org/10.1007/s10549-008-9937-0.
16. Shapiro, C.L, Manola, J., Leboff, M. Ovarian failure after adjuvant chemotherapy is associated with rapid bone loss in women with early-stage breast cancer.
17. 2019 ISCD Official Positions – Adult-International Society for Clinical Densitometry (ISCD). (2019) Iscd.Org. https://www.iscd.org/officialpositions/2019-iscd-official-positions-adult
18. Jang, H. D., Hong, J. Y., Han, K., Lee, J. C., Shin, B. J., Choi, S. W., Suh, S. W., Yang, J. H., Park, S. Y., & Bang, C. (2017). Relationship between bone mineral density and alcohol intake: A nationwide health survey analysis of postmenopausal women. PloS one, 12(6), e0180132. https://doi.org/10.1371/journal.pone.0180132

Pre-trained Convolutional Neural Networks in the Assessment of Bone Scans for Metastasis

Vincent Peter C. Magboo, MD, MS[1, 2], Ma. Sheila A. Magboo, MS[1]

[1] *Department of Physical Sciences and Mathematics, University of the Philippines Manila*

[2] *Section of Nuclear Medicine, University of Perpetual Help Medical Center*

E-mail address: vcmagboo@up.edu.ph, mamagboo@up.edu.ph

ABSTRACT

Background:

Numerous applications of artificial intelligence have been applied in radiological imaging ranging from computer-aided diagnosis based on machine learning to deep learning using convolutional neural networks. One of the nuclear medicine imaging tests being commonly performed today is bone scan. The use of deep learning methods through convolutional neural networks in bone scintigrams has not been fully explored. Very few studies have been published on its diagnostic capability of convolutional neural networks in assessing osseous metastasis.

Objective:

The aim of our study is to assess the classification performance of the pre-trained convolutional neural networks in the diagnosis of bone metastasis from whole body bone scintigrams of a local institutional dataset.

Methods:

Bone scintigrams from all types of cancer were retrospectively reviewed during the period 2019-2020 at the University of Perpetual Help Medical Center in Las Pinas City, Metro Manila. The study was approved by the Institutional Ethical Review Board and Technical Review Board of the medical center. Bone scan studies should be mainly for metastasis screening. The pre-processing techniques consisting of image normalization, image augmentation, data shuffling, and train-test split (testing at 30% and the rest (70%) was split 85% for training and 15% for validation) were applied to image dataset. Three pre-trained architectures (ResNet50, VGG19, DenseNet121) were applied to the processed dataset. Performance metrics such as accuracy, recall (sensitivity), precision (positive predictive value), and F1-scores were obtained.

Results:

A total of 570 bone scan images with dimension 220 x 646 pixel sizes in .tif file format were included in this study with 40% classified with bone metastasis while 60% were classified as without bone metastasis. DenseNet121 yielded the highest performance metrics with an accuracy rate of 83%, 76% recall, 86% precision, and 81% F1-score. ResNet50 and VGG19 had similar performance with each other across all metrics but generally lower predictive capability as compared to DenseNet121.

Conclusion:

A bone metastasis machine learning classification study using three pre-trained convolutional neural networks was performed on a local medical center bone scan dataset via transfer learning. DenseNet121 generated the highest performance metrics with 83% accuracy, 76% recall, 86% precision and 81% F1-score. Our simulation experiments generated promising outcomes and potentially could lead to its deployment in the clinical practice of nuclear medicine physicians. The use of deep learning techniques through convolutional neural networks has the potential to improve diagnostic capability of nuclear medicine physicians using bone scans for the assessment of metastasis.

***Keywords**: Deep Learning, Convolutional Neural Networks, Transfer Learning, Bone Metastasis*

INTRODUCTION

In the recent years, numerous applications of artificial intelligence (AI) have been applied in radiological imaging ranging from computer-aided diagnosis based on machine learning to deep learning using convolutional neural networks (CNN) [1]. Deep learning techniques have been studied for various potential applications such as data acquisition, image reconstruction and image registration, image segmentation, image classification and lesion segmentation [2]. The seeming endless applications in radiological imaging being considered a data-rich medical specialty have been made possible due to the advances and widespread availability not only in hardware but in software as well [3]. However, for many radiologists and nuclear medicine physicians, the term AI appears to be a blackbox with doubts on its interpretability and perceived as a threat to their clinical practice [4].

One of the nuclear medicine imaging tests commonly performed today is bone scan. Its primary indication is to detect the presence of osseous metastasis which would then suggest that the cancer has reached its advanced stage with a median survival of a few months and having limited appropriate therapies [5, 6]. Many cancers, like breast, prostate, and lung malignancies are known to spread to the bones. In 25-40% of advanced breast cancer patients, bones are usually the first site of distant metastasis [7]. In prostate cancer, the metastatic deposits in the axial skeleton can cause pain, debility and/or functional impairment impacting the quality of life of the patients [8].

The use of CNN in bone scintigrams has not been fully explored. Very few studies have been published on the diagnostic capability of CNN in assessing osseous metastasis. Papandrianos et al developed a robust CNN architecture for bone metastasis diagnosis using whole - body scan images with an impressive classification accuracy of 92.50% besting other popular and well-known CNN architectures for medical imaging like ResNet50, VGG16, MobileNet, and DenseNet [6]. Using a meticulous exploration of CNN hyperparameter selection and fine-tuning, Papandrianos et al, applied a CNN model for the classification of bone scans for metastasis among prostate cancer patients. The model yielded classification testing accuracy of 97.38% outperforming VGG16, ResNet50, GoogleNet, and MobileNet [9]. In another study involving 14,972 bone lesions from whole - body bone scans the authors compared a 2D CNN based on the RestNet50 architecture with InceptionV3, VGG16, and DenseNet169. Results showed their CNN model bested other pre-trained architectures with an average sensitivity, specificity, accuracy, positive predictive value, and negative predictive value for all visible bone lesions at 81.30%, 81.14%, 81.23%, 81.89%, and 80.61%, respectively [10]. In a masteral thesis by Dang, the author designed a CNN to classify hotspots in bone scintigram for bone metastasis with a testing accuracy rate of 89% [11].

OBJECTIVE

The aim of our study is to assess the classification performance of the pre-trained convolutional neural networks in the diagnosis of bone metastasis from whole body bone scintigrams of a local institutional dataset. The performance metrics include accuracy, precision, recall and F1-score.

MATERIALS AND METHODS

Bone scintigrams during the period 2019-2020 at the University of Perpetual Help Medical Center in Las Pinas City, Metro Manila were retrospectively reviewed. The study was approved by the Institutional Ethical Review and Technical Review Boards of the medical center and was conducted in accordance with the Declaration of Helsinki for the ethical conduct of research involving human participants. The machine learning pipeline for this study is shown in Figure 1.

Characteristics of Dataset

Bone scintigrams from all types of cancers during the period 2019-2020 of the medical center were included in the study. The bone scan studies should be mainly for metastasis screening. Other indications of bone scans such as assessment of metabolic bone disease, osteomyelitis versus cellulitis, loosening of implants/ prosthesis, identification of primary bone tumors, etc. were excluded in the study.

Bone scan images consisted of whole body anterior and posterior views with 1024 x 256 pixel resolution. All bone scan procedures were performed with a Siemens

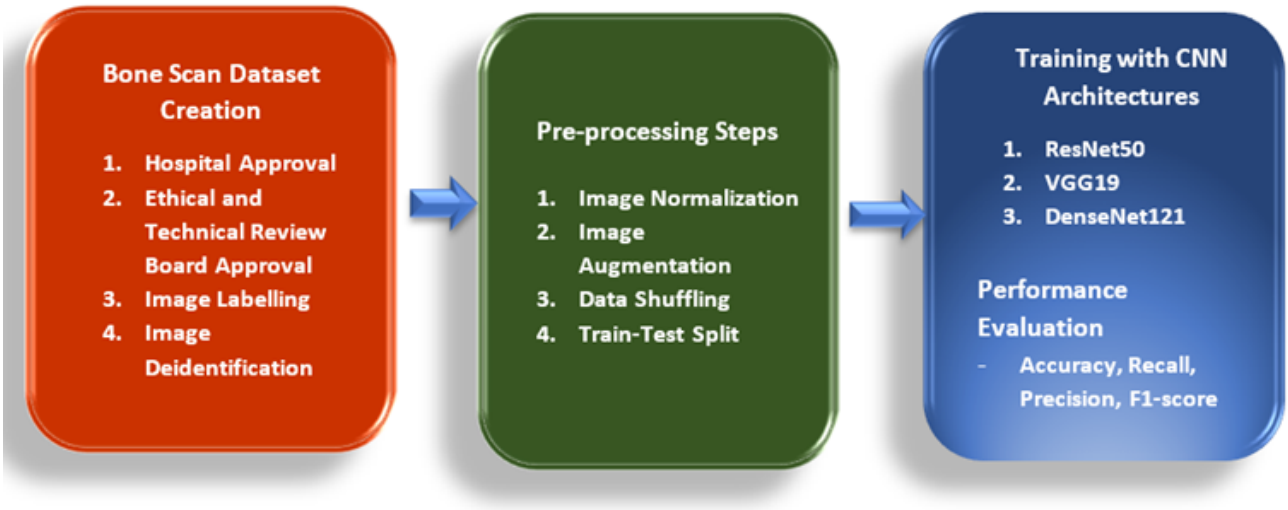

FIGURE 1. Machine Learning Pipeline for Bone Metastasis Study

gamma camera Symbia S series with two heads, with low energy high resolution collimators (LEHR), and with SyngoVE32B software. Bone scans were obtained 3 hours after the intravenous administration of 25 - 30 mCi of technetium-99m methylene diphosphonate (Tc-99m MDP) using a low-energy high-resolution collimator, matrix size of 1024 x 256, an acquisition time of 15 – 20 cm/min and photon energy centered on the 140-keV photo-peak with a symmetrical 20% energy window [12, 13]. The scanning procedure was in accordance with the guidelines set by the European Association of Nuclear Medicine and Society of Nuclear Medicine.

Labelling of Images

The interpretation of bone scan images was performed by a board-certified nuclear medicine physician with almost 25-year clinical experience in bone scan interpretation. Quality assurance of all the images before its inclusion in the machine learning pipeline was made. A pre-processing approach was also done to remove artifacts (non-osseous uptake such as urine contamination, site of tracer injection etc) in the original images. Images with medical devices such as implant, catheters etc were also excluded in the study to avoid interference with image interpretation. Additionally, all included bone scan whole body images underwent deidentification procedure resulting to cropped images for inclusion in the study. Images were then classified into two classes: (1) with scintigraphic evidence of bone metastasis and (2) without scintigraphic evidence of bone metastasis. The following were used as the criteria for the scintigraphic evidence of bone metastasis: (a) based on the typical patterns of tracer uptake seen in metastasis, (b) interval appearance of new bone lesions that cannot be ruled out as malignant in follow-up scans, (c) presence of flare phenomenon on scans, (d) when the accompanying medical records and radiological reports (CT scan, radiographs, MRI, PET/CT, bone alkaline phosphatase elevation) indicate bone destruction, and (e) when bone lesions appeared enlarged after at least 3 months follow-up. On the other hand, following criteria were used to classify bone scan as without scintigraphic evidence of bone metastasis: (a) bone lesions confirmed to be traumatic in origin, (b) lesions whose tracer uptake appeared around the bone joint, (c) lesions which the accompanying radiological studies indicate non-osseous metastasis and (d) equivocal lesions which lack definitive evidence of metastasis. Figure 2 shows a sample image indicating with and without bone metastasis

Pre-Processing Techniques

Numerous pre-processing techniques were applied to image dataset. These consisted of (a) image normalization using Min-Max normalization, (b) image augmentation, c) data shuffling for random order of the datset, and (d) data train-test split. The dataset was split in three parts: testing (30%) and the rest (70%) is split 85% for training and 15% for validation. The following geometric augmentations were applied to all images: (1) zoom range, (2) horizontal flipping, (3) rotation range, (4) translation, and (5) shear range.

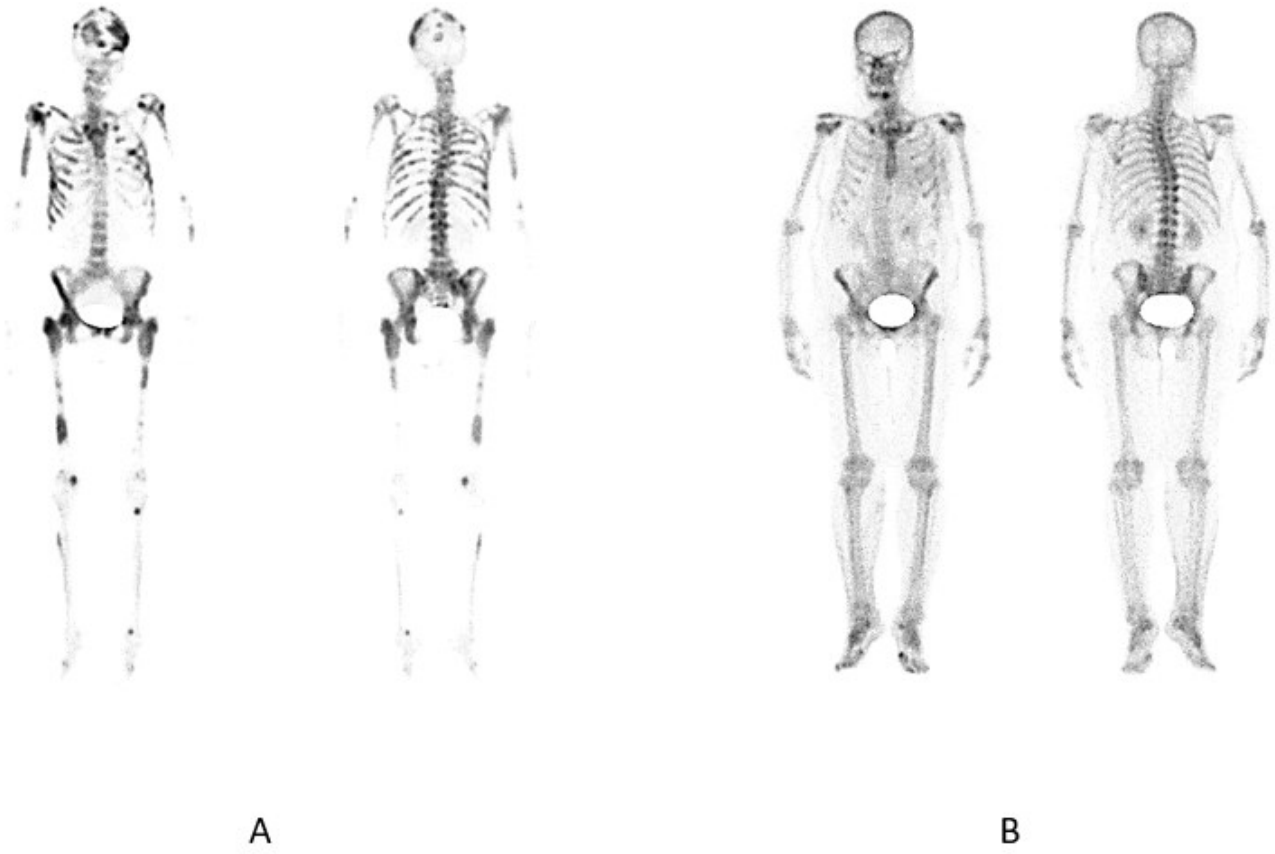

FIGURE 2. Sample bone scan image (A) with bone metastasis and (B) without bone metastasis

Architecture of the Convolutional Neural Networks

Popular pre-trained CNNs typically used in medical imaging were applied to the processed dataset. These include ResNet50, VGG19, and DenseNet121. ResNet50 is a CNN model consisting of 50 layers version of ResNet (Residual Neural Network) trained on ImageNet database. Its architecture consists of sequences of convolutional blocks with average pooling and uses softmax at the last layer for classification [14, 15, 16, 17]. VGG-19 is one of the VGG (Visual Geometry Group) based architectures with 19 connection layers, including 16 convolution layers and 3 fully connected layers. The convolution layers extract features of the input images, the fully connected layers with softmax make the final classification and uses Maxpooling instead of average pooling for downsampling to reduce volume size prior to classification [15, 17, 18, 19]. DenseNet (Dense Convolutional Neural Network) is another type of CNN architecture commonly employed for visual object recognition. DenseNet121 consists of 121 layers with parameters of more than 8 million, divided into DenseBlocks. The layers between the blocks are called transition layers and uses a batch normalization for down-sampling and employ softmax activation function in the last fully connected layer for the classification [16, 20, 21]. Huan et al have reported the advantages of DenseNet121 as follows: alleviation of the vanishing-gradient problem, strengthening of the feature propagation, encourage feature reuse, and substantial reduction of the number of parameters [20]. The architecture of these pre-trained CNN's are shown in Figures 3 - 6.

All simulation experiments were performed in Kaggle as it supports free use of NVIDIA TESLA P100 GPUs. Keras 2.6.0, TensorFlow 2.6.0., and python language 3.7.10 were utilized in all simulations.

Performance Metrics

Performance of the pre-trained architectures in the classification of bone metastasis, accuracy, recall (sensitivity), precision (positive predictive value), and F1 scores were computed.

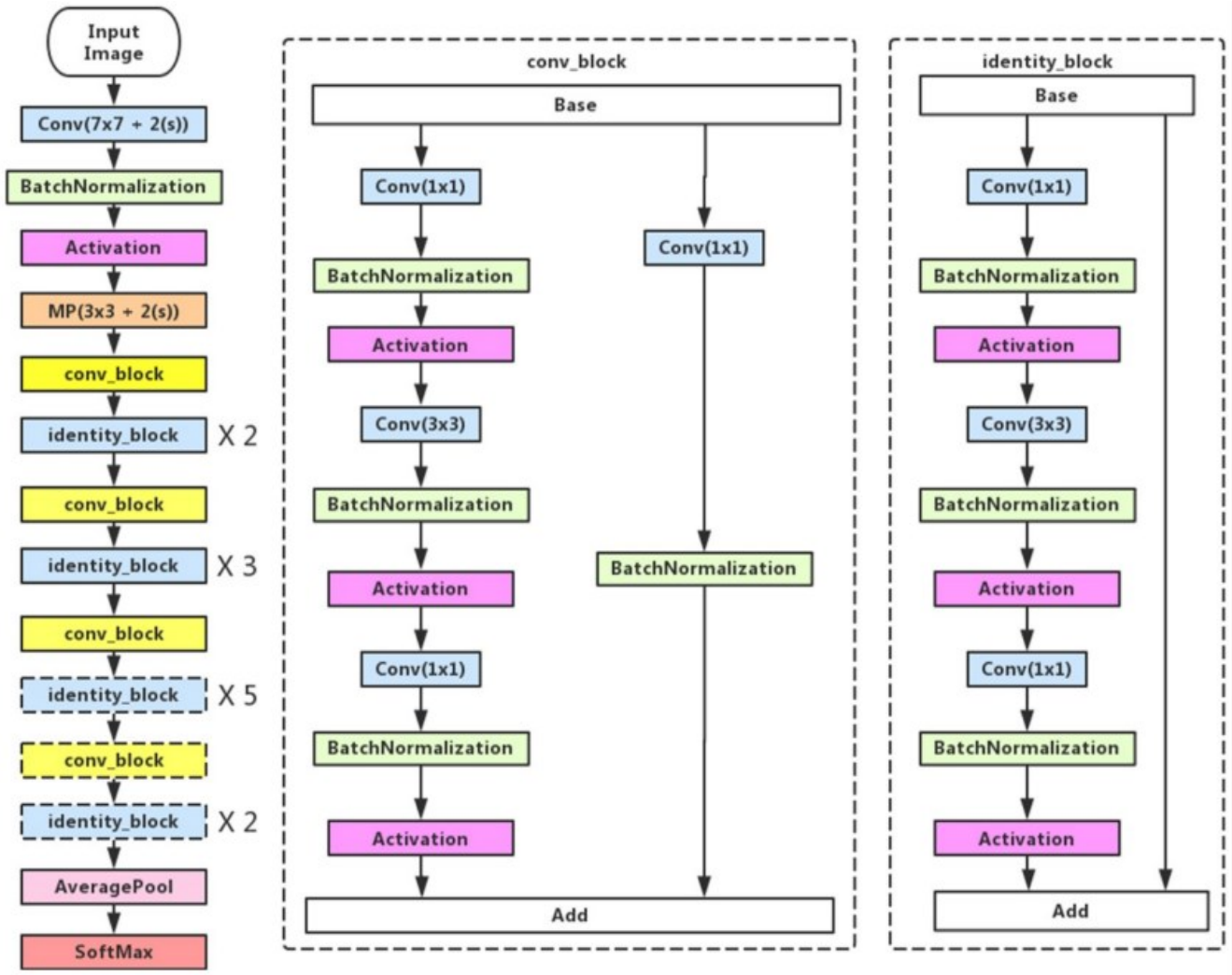

FIGURE 3. ResNet50 Architecture (Source:[14])

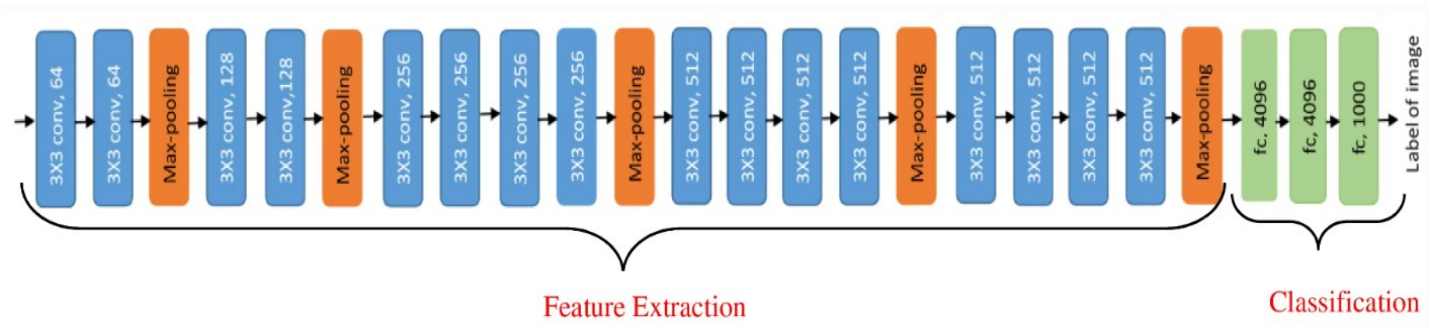

FIGURE 4. VGG19 Architecture (Source:[19])

RESULTS

Included in this study were 570 bone scan images with dimension 220 x 646 pixel sizes in .tif file format of which 228 (40%) images were classified with bone metastasis while 342 (60%) images were classified as without bone metastasis. Majority of our cases were females at 68% with breast cancer as the most common type of malignancy. The clinical characteristics of bone scan patients is seen in Table 1.

DenseNet121 yielded the highest performance metrics with an accuracy rate of 83%, 76% recall (sensitivity), 86% precision (positive predictive value), and 81% F1 - score. ResNet50 and VGG19 had similar performance with each other across all metrics but generally lower predictive capability as compared to DenseNet121. The performance metrics of each architecture are shown in Figure 6.

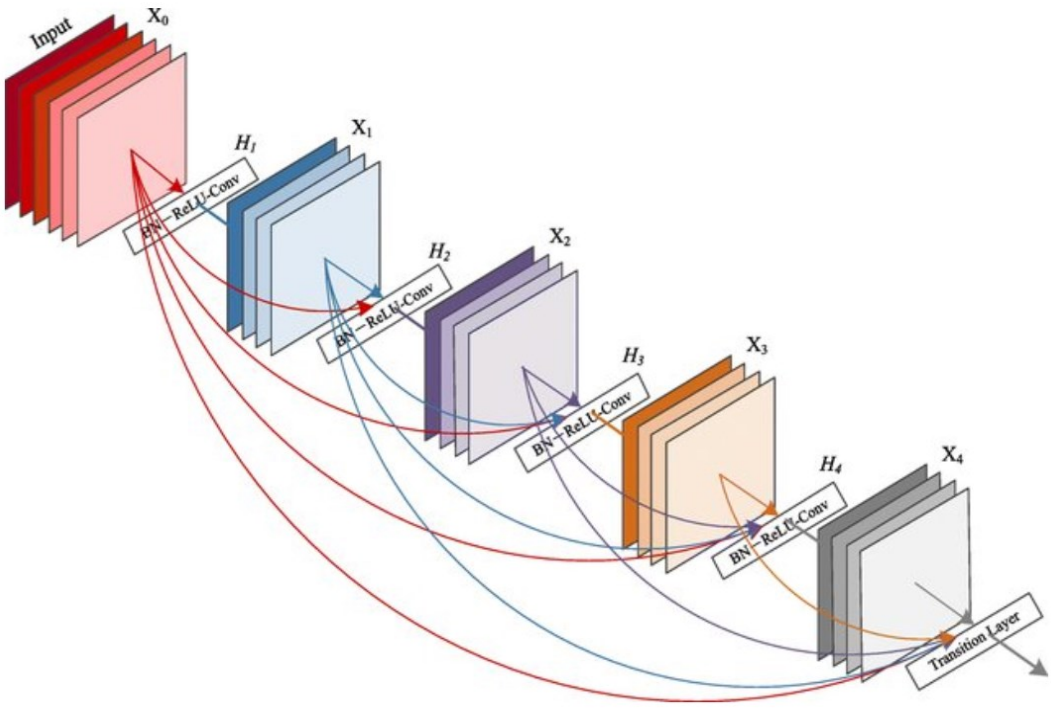

FIGURE 5. DenseNet121 Architecture (Source:[20])

DISCUSSION

We have conducted simulation experiments on a bone scan dataset of a local medical center. All bone scan images underwent data cleaning for quality assurance. This was followed by application of pre-processing techniques in an attempt to increase the predictive capability of CNN models as well as avoidance of potential overfitting. The use of geometric augmentation is a standard practice in machine learning as it improves the performance of CNN models in image classification. In our study, DenseNet121 showed the highest predictive performance as compared to the VGG19 and ResNet50. As compared to other studies reported in the literature showing good performance of various pre-trained architectures in the classification of osseous metastasis from bone scans, our results are generally lower [6,9,10,19]. This could be brought about by the relatively small number of images included in our dataset. Nonetheless, our results are similar to that of Papandrianos et al [6], which showed DenseNet121 with the highest performance.

Pre-trained CNN models are trained on numerous datasets with various categories of images. However, these are not trained on radiological images. However, transfer learning techniques can still employ these pre - trained models on a variety of computer vision problems. This is more particularly prominent in areas with limited resources (dataset and computing resources). The availability of labelled radiological images for deep learning studies are very few. In the Philippines, we believe this study is the first its kind in applying machine learning techniques in nuclear medicine images.

While the pre-trained CNN models have fairly - satisfactory performance metrics rates suitable for use in clinical practice, DenseNet121 obtained the highest predictive capability for classifying osseous metastasis. Hence, DenseNet121 can be tapped by nuclear medicine physicians as a decision support tool in the interpretation of bone scintigrams. Complementing bone scan (with well-known excellent sensitivity) with the use of these CNN models due to its positive predictive value highlights the potential utility of CNN models in the clinical practice of nuclear medicine physicians.

CONCLUSIONS

A bone metastasis machine learning classification study was performed on a local medical center bone scan dataset via transfer learning. Three pre-trained convolutional neural networks were assessed for its capability to detect bone metastasis from bone scans. DenseNet121 generated the highest performance metrics with 83% accuracy, 76% recall, 86% precision

TABLE 1. Clinical Characteristics of Bone Scan Patients

Clinical Features	Percentage (%)
Male	**32%**
Female	**68%**
Age (years)	**46.55 ± 8.12**
Type of Malignancy	
Breast Cancer	**70 %**
Prostate Cancer	**15 %**
Lung Cancer	**2 %**
GI Malignancies (Colon,	**2 %**
Rectal, Anal, Appendiceal)	**1 %**
Other Malignancies	
Labelled Images (570 images)	
With bone metastasis	**228 (40%)**
Without bone metastasis	**342 (60%)**

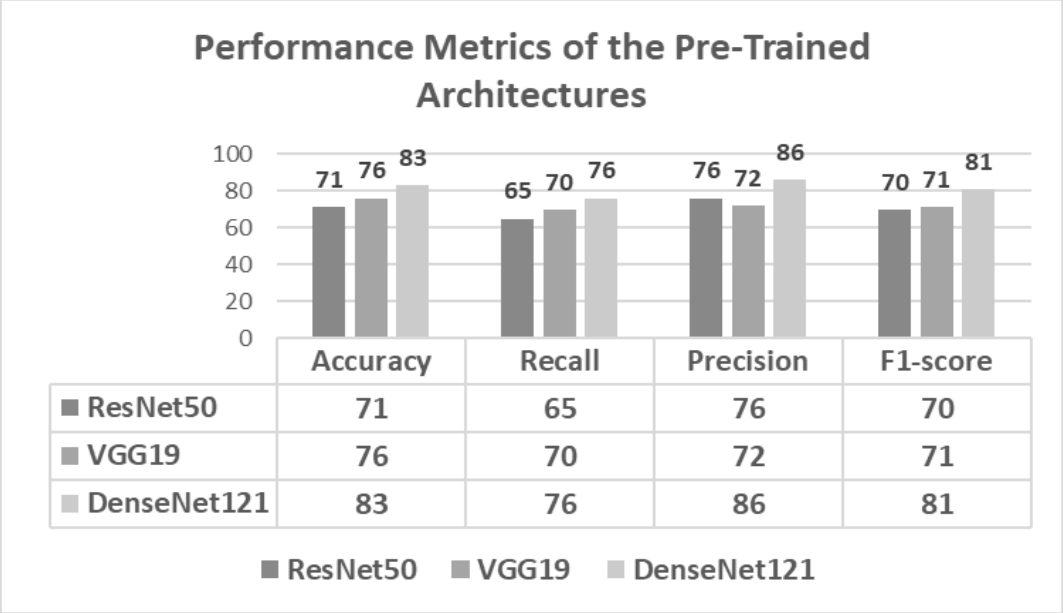

FIGURE 6. Forest Performance Metrics of the Pre-Trained Architectures

and 81% F1-score. Our simulation experiments generated promising outcomes and potentially could lead to its deployment in the clinical practice of nuclear medicine physicians. The use of deep learning techniques through convolutional neural networks has the potential to improve diagnostic capability of nuclear medicine physicians using bone scans for the assessment of metastasis.

RECOMMENDATIONS

Addition of more bone scan images is highly recommended to improve the performance of the neural network models as deep learning techniques generally require huge amount of images. Additionally, it is highly recommended to do more simulations with other pre-trained architectures, using different learning rates and different types of optimizers.

REFERENCES

1. Mun SK, Wong KH , Lo SCB, Li Y, Bayarsaikhan S. "Artificial Intelligence for the Future Radiology Diagnostic Service". Frontiers in Molecular Biosciences, Vol 7, 2021. https://www.frontiersin.org/articles/10.3389/fmolb.2020.614258.
2. Wang S, Cao G, Wang Y, Liao S, Wang Q, Shi J, Li C, Shen D. "Review and Prospect: Artificial Intelligence in Advanced Medical Imaging". Frontiers in Radiology, Vol 1, 2021. https://www.frontiersin.org/articles/10.3389/fradi.2021.781868

3. Sala E, Ursprung, S. “Artificial Intelligence in Radiology: The Computer’s Helping Hand Needs Guidance”. Radiology: Artificial Intelligence, vol 2 (6), pe200207, 2020. doi = 10.1148/ryai.2020200207.
4. Nensa F, Demircioglu A, Rischpler C. “Artificial Intelligence in Nuclear Medicine”. J Nucl Med 2019; 60:29S–37S. DOI: 10.2967/jnumed.118.220590.
5. Valenti MT, Mottes M, Carbonare LD, Feron O. “Editorial: Bone Metastases”. Frontiers in Oncology, vol 11, 3030, 2021. https://www.frontiersin.org/article/10.3389/fonc.2021.741515.
6. Papandrianos N, Papageorgiou E, Anagnostis A, Feleki A. “A Deep-Learning Approach for Diagnosis of Metastatic Breast Cancer in Bones from Whole-Body Scans”. Applied Sciences. 2020; 10(3):997. https://doi.org/10.3390/app10030997.
7. Murat K, Baha Z, Raika D, Funda T, Zehra A, Cenk S, Adam U. “Clinicopathologic features of single bone metastasis in breast cancer”. Medicine. 100, 1, e24164, 2021. DOI: https://doi.org/10.1097/MD.0000000000024164.
8. Mingyu Z, Xin L, Yuan Q, Silong H, Yingjian Z, Wentao L, et al. “Bone metastasis pattern of cancer patients with bone metastasis but no visceral metastasis”. J Bone Oncol. 2019 Apr 15. https://www.ncbi.nlm.nih.gov/pmc/articles/PMC6357895/.
9. Papandrianos N, Papageorgiou E, Anagnostis A, Papageorgiou K. “Bone metastasis classification using whole body images from prostate cancer patients based on convolutional neural networks application”. PLoS ONE 15(8): e0237213, 2020. https://doi.org/10.1371/journal.pone.0237213.
10. Liu Y, Yang P, Pi Y, Jiang L, Zhong X, Cheng J, Xiang Y, Wei J, Li L, Yi Z, Cai H, Zhao Z. “Automatic identification of suspicious bone metastatic lesions in bone scintigraphy using convolutional neural network”. BMC medical imaging, 21(1), 131, 2021. doi: https://doi.org/10.1186/s12880-021-00662-9.
11. Dang, J. Classification in Bone Scintigraphy Images Using Convolutional Neural Networks. Master’s Thesis, Lund University, Lund, Sweden, 2016.
12. den Wyngaert TV, Strobel K, Kampen WU, Kuwert T, van der Bruggen W, Mohan H, Gnanasegaran G, Delgado-Bolton R, Weber W, Beheshti M, Langsteger W, Giammarile F, Mottaghy F, Paycha F, and EANM Bone & Joint Committee and the Oncology Committee. 2016. “The EANM practice guidelines for bone scintigraphy”. European journal of nuclear medicine and molecular imaging, 43, 9, 1723–1738, 2016. doi: https://doi.org/10.1007/s00259-016-3415-4.
13. Bartel T, Kuruva M, Gnanasegaran G, Beheshti M, Cohen E, Weissman A, and Yarbrough T. “SNMMI Procedure Standard for Bone Scintigraphy 4.0”. Journal of nuclear medicine technology, 46, 4, 398–404, 2018. doi: https://tech.snmjournals.org/content/46/4/398.
14. Ji Q, Huang J, He W, Sun Y. “Optimized Deep Convolutional Neural Networks for Identification of Macular Diseases from Optical Coherence Tomography Images”. Algorithms, 12(3):51, 2019. https://doi.org/10.3390/a12030051.
15. Ikechukwu AV, Murali S, Deepu R, Shivamurthy RC. “ResNet-50 vs VGG-19 vs training from scratch: A comparative analysis of the segmentation and classification of Pneumonia from chest X-ray images”. Global Transitions Proceedings, 2(2), Issue 2 375-381, 2021. https://doi.org/10.1016/j.gltp.2021.08.027.
16. Shazia, A., Xuan, T.Z., Chuah, J.H. et al. A comparative study of multiple neural network for detection of COVID - 19 on chest X-ray. EURASIP J. Adv. Signal Process. 2021, 50 (2021). https://doi.org/10.1186/s13634-021-00755-1.
17. Ali L, Alnajjar F, Jassmi, HA, Goocho M, Khan W, Serhani MA. “Performance Evaluation of Deep CNN - Based Crack Detection and Localization Techniques for Concrete Structures.” Sensors 21, 1688, 2021. https://doi.org/10.3390/s21051688.
18. Simonyan K, Zisserman A. “Very deep convolutional networks for large-scale image recognition”. 3rd Int. Conf. Learn. Represent. ICLR 2015 - Conf. Track Proc (2015), pp. 1-14.
19. Bansal, M., Kumar, M., Sachdeva, M. et al. Transfer learning for image classification using VGG19: Caltech-101 image data set. J Ambient Intell Human Comput (2021). https://doi.org/10.1007/s12652-021-03488-z.
20. Huang G, Liu Z, Van Der Maaten L, Weinberger KQ. "Densely Connected Convolutional Networks," 2017 IEEE Conference on Computer Vision and Pattern Recognition (CVPR), Honolulu, HI, USA, 2017, pp. 2261-2269, doi: 10.1109/CVPR.2017.243.
21. Hasan, N., Bao, Y., Shawon, A. et al. DenseNet Convolutional Neural Networks Application for Predicting COVID-19 Using CT Image. SN COMPUT. SCI. 2, 389 (2021). https://doi.org/10.1007/s42979-021-00782-7.
22. Ntakolia C, Diamantis D, Papandrianos N, Moustakidis S, Papageorgiou E. “A Lightweight Convolutional Neural Network Architecture Applied for Bone Metastasis Classification in Nuclear Medicine: A Case Study on Prostate Cancer Patients.” Healthcare (Basel, Switzerland), 8, 4, 493, 2020. DOI: https://doi.org/10.3390/healthcare8040493.

PET-Positron Emission Production System

Radiochemistry System

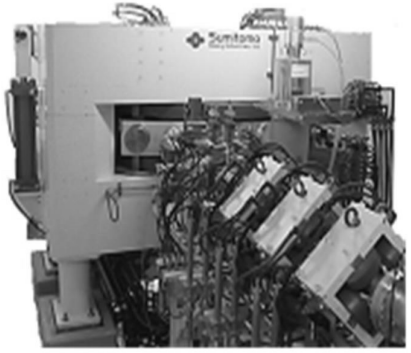

Other RI Production System

NUCLEAR MEDICINE

Tc99m Generator

Radiopharmaceuticals

Sealed Sources

Hot laboratory set-up and accessories

RIA/IRMA Kits

Sumitomo Heavy Industries, Ltd.

PROTECH Medical

Assurance Controls Technologies

Assurance Controls Technologies Co., Inc.

Manila ~ Cebu ~ Davao +6327244149, +6327244150, +6327224580, +6327224588

MERCK

ALWAYS CURIOUS

IMAGINE

THE NEXT 350 YEARS

Molecular Imaging

See a whole new world of precision

Expanding precision medicine

Answering to clinical needs in oncology, neurology, cardiology, and radiology, Siemens Healthineers Molecular Imaging systems provide Biograph Vision PET/CT and Symbia Intevo Bold SPECT/CT solutions to help clinicians diagnose, treat, and monitor disease more confidently.

With AIDAN, the new Biograph PET/CT scanner platform, allows you to perform PET/CT exams with ease. It helps you become more efficient and personalized yet standardized. All this, with the click of a button.

xSPECT™ technology, completely integrates SPECT and CT data during image reconstruction for sharp clinical detail and accurate measurement of disease.

siemens-healthineers.com/molecular-imaging

SIEMENS Healthineers